

Radar scattering in an alpine glacier: Evidence of seasonal development of temperate ice beneath ogives

John H. McBride¹, Summer B. Rupper¹, Scott M. Ritter¹, David G. Tingey¹, Michelle R. Koutnik², Annika M. Quick¹, Thomas H. Morris¹, R. William Keach II¹, Landon K. Burgener¹, Adam P. McKean¹, Jessica Williams¹, Joshua M. Maurer¹, Durban G. Keeler¹, and Robert Windell¹

¹Department of Geological Sciences, Brigham Young University, P.O. Box 24606, Provo, Utah 84602, USA

²Centre for Ice and Climate, Niels Bohr Institute, University of Copenhagen, Juliane Maries Vej 30, DK-2100-Copenhagen, Denmark

ABSTRACT

Glacial ogives are transverse topographic, wave-like surface features that form below icefalls on some alpine glaciers. Ground-penetrating radar surveys from the Gorner glacier system in the Swiss Alps reveal an along-flow periodicity in scattering intensity that correlates with ogives. The scattering appears in the ablation zone and occurs at 5–20 m depth. The geometry of the scattering mimics that of the ogives, although exaggerated in amplitude. We interpret the scattering to represent lateral variations in water content. We propose that as glacial ice accelerated and stretched through the icefall, seasonal fluctuations occurred in water infiltration to crevasses during the summer and subsequent freezing of that water in the crevasses in the winter. This seasonally varying infilling and freezing locally altered the distribution of temperature, creating zones of temperate ice with water inclusions that preferentially scatter radar energy. In addition to the scattering pattern, highly reflective planar features associated with these periodic regions of temperate ice are interpreted as water-filled fractures. A three-dimensional rendering of the orientation of these planar features precludes a “fold-and-thrust” hypothesis for the formation of the ogives.

INTRODUCTION

Glacial ogives are a classic feature of some alpine glaciers and have been studied for well over 100 years, yet they remain one of the most puzzling features of glacial ice (Fisher, 1962; Posamentier, 1978; Waddington, 1986; Hambrey and Lawson, 2000; Goodsell et al., 2002). The term ogive, used in architecture and engineering to mean a pointed arch, refers to a periodic expression of either banded color changes

caused by rock debris or an undulating wave expressed on the glacier surface. Wave ogives initially develop seasonally just below the icefall as a series of surface undulations with an amplitude of several meters (one wavelength is thought to be equivalent to 1 year of glacial flow; Nye, 1958; Waddington, 1986). Band ogives may represent the distal extent of eroded wave ogives, with only bands of alternating debris remaining (Cuffey and Paterson, 2010).

In a seminal study, Goodsell et al. (2002) used surface-deployed radar to reveal a prominent subsurface periodic scattering structure in the alpine glacier Bas Glacier d’Arolla in southern Switzerland that correlated with band ogives on the surface. A similar structure was observed by McBride et al. (2010) along a small portion of a tributary glacier of the Gornergletscher system, the Zwillingsgletscher, which has wave ogives and is located ~25 km southeast of the Bas Glacier d’Arolla. Further, a radar and deep-drilling study by Eisen et al. (2009) of the Gornergletscher system drew an association between zones of radar scattering and water inclusion (or temperature). Questions raised by these studies include: why does the radar scattering show a periodic pattern and how does the glacial thermal structure interact with fractures in the ice to possibly influence this pattern? In this paper, we further examine this subsurface structure with surface-deployed radar, which leads us to answer these questions.

Two mechanisms are widely cited for ogive formation (mainly focused on band ogives), the shearing hypothesis (Posamentier, 1978) and the “summer versus winter passage” hypothesis (Nye, 1958; summarized by Appleby et al., 2010; for a review of the differing mechanisms, see Goodsell et al., 2002). The “summer versus winter passage” hypothesis states that as ice accelerates across the icefall zone, it is stretched. In addition, ice passing through in summer loses more ice by ablation than during the winter (Nye,

1958). Together, these processes result in wave ogives at the base of the icefall. Posamentier (1978) proposed what is now a classic “fold-and-thrust–style” geological model for ogive development in which deep debris-laden ice is thrust over near-surface ice with less debris, thus forming periodic band ogives. This model postulates that as the ice flows down the glacier from the icefall accumulation zone, shear zones deform the ice into tight, asymmetric folds. These folds are truncated by reverse faults verging in the down-glacier direction. Goodsell et al. (2002) invoked this shearing model to explain the ogive-related radar scattering pattern observed on the Bas Glacier d’Arolla. Similarly, Appleby et al. (2010) interpreted band ogives on the Fox glacier to be formed by multiple thrust zones that brought deeper, banded ice to the surface.

Over the past decade, surface-deployed radar has been increasingly used to study the internal structure of glaciers, taking advantage of the low attenuation of electromagnetic waves in solid ice (e.g., Matsuoka et al., 2010). Numerous studies have demonstrated that the interior of a glacier may strongly scatter radar energy (e.g., Woodward and Burke, 2007; Bradford et al., 2009; Eisen et al., 2009). Water-filled voids or rock debris have been hypothesized to be the cause of such scattering (e.g., Bamber, 1988; Moorman and Michel, 2000; Gusmeroli et al., 2010; see also Lawson et al., 1998; Arcone et al., 2000). The dominant point of view is that the onset of water causes the onset of radar scattering (e.g., Björnsson et al., 1996). However, such studies have usually not attempted to correlate radar scattering with surface features of a glacier (e.g., the topographic variation in the ice surface, including ogives). Thus, the relation of scattering to the dynamic processes that affect the overall ice structure and development has not been well established. In this paper, we explore the spatial relation between the ogive topographic pattern and internal radar scatter-

ing on the Gornergletscher system located in the Alps of south-central Switzerland (Canton Valais). Our purpose is to find the cause of the unusual periodic scattering structure observed in some alpine glaciers with ogives. We test the hypothesis that periodic scattering associated with ogives represents seasonal episodes where crevasses fill with water during the spring and summer and subsequently freeze during the fall and winter, causing latent heating of the surrounding ice during the colder seasons. If this is correct, then from summer to fall, the crevasse-zone ice is thermally altered, resulting in pockets of temperate ice during the colder seasons. Further, maximum subsurface scattering should correlate with the gradient of ogive topography. In this paper, we interpret the intensity and distribution of scattering to represent different thermal zones in the ice that form due to a combination of fracturing, permeability, and latent heat release due to infiltration and freezing of liquid water.

We acquired radar profiles at multiple frequency bands, and topographic surveys within the ablation zones of the Zwillingsgletscher and the Grenzgletscher (branches within the Gornergletscher system) (Fig. 1). Our objectives were to acquire subsurface images of not only the main trunk of the Zwillingsgletscher (in the direction of glacial flow), but also orthogonal sections (perpendicular to glacial flow) using both two-dimensional (2-D) and three-dimensional (3-D) strategies in order to examine radar scattering and fracturing in detail. Topographic surveys accompanied the radar surveys in order to tie ogive waves to the radar scattering structure. In the context of our findings, we review previous studies (e.g., Bamber, 1988; Björnsson et al., 1996; Bradford and Harper, 2005; Eisen et al., 2009) where radar scattering has been related to water (and temperature) or rock debris content. We invoke a similar explanation for our scattering observations, and discuss how the scatterers likely were generated. Our work is in line with recent studies that have begun to explore how water within the ice may affect the movement of alpine glaciers and ice sheets (e.g., by reducing internal friction) (Fountain et al., 2005; Harper et al., 2010; Schoof, 2010; Bælum and Benn, 2011). In addition, thermal properties of ice are well known to strongly influence ice rheology, and thus glacier flow (Cuffey and Paterson, 2010).

STUDY AREA

The Gornergletscher system in the Swiss Alps (Figs. 1 and 2) represents the confluence of five tributary glaciers, some of which form wave ogives down-glacier of icefalls. Wave ogives

can be readily observed on satellite imagery (Fig. 1D) as a periodic ribbed pattern that decreases in wavelength down the glacier (i.e., to the northwest). These ogives clearly show that the physical properties of ice originating at and modified through the icefall are maintained far down glacier from their source (e.g., Fisher, 1962; Waddington, 1986). The particular ogives of interest form at the icefall of the Zwillingsgletscher and extend more than a kilometer down glacier (Fig. 3) from the confluence of the Zwillingsgletscher and Grenzgletscher (Fig. 1).

The Gornergletscher system is one of the more thoroughly studied alpine valley glacial systems (Eisen et al., 2009; Walter et al., 2010). Previous radar investigations in Canton Valais have concentrated on the Grenzgletscher (the eastern branch of the Gornergletscher system) (Eisen et al., 2009) and on the Bas Glacier d'Arolla (Goodsell et al., 2002), located ~25 km west of our study area. Very different radar patterns and glacial morphologies have been reported for the two glaciers. The Grenzgletscher covers a broad area and is several hundred meters thick (Eisen et al., 2009). This glacier lies between the Gornergletscher proper to the northeast and the Zwillingsgletscher to the southwest (Figs. 1 and 2). Borehole thermometry on the Grenzgletscher indicates a thick layer of cold ice, which partially correlates with a zone of low radar scattering (using 1–5 and 40 MHz antennas), underlain by a strongly scattering layer, approximately correlating with warmer ice (Eisen et al., 2009). In contrast, the Bas Glacier d'Arolla is an isolated glacier, occupying a narrow valley. No temperature-depth profiles have been reported for the Bas Glacier d'Arolla, but radar images (using a 100 MHz antenna) show a distinct pattern of radar scattering having a periodic shape with an onset at ~5 m (for a velocity of 0.167 m/ns) below the ice surface (Goodsell et al., 2002). The radar images are transparent above this onset. As reported by Goodsell et al. (2002), the Bas Glacier d'Arolla has well-developed banded ogives but no wave ogives.

Our study focuses on the Zwillingsgletscher, which is a narrow (~200–500 m wide in our study area) valley glacier like the Bas Glacier d'Arolla, but which is several kilometers long and forms a confluence within the larger Gornergletscher system lying to the northeast (Fig. 2). Further, the flow dynamics of the Zwillingsgletscher are undoubtedly influenced by the Grenzgletscher against which it abuts, and the Schwärzegletscher with which it forms a confluence further down glacier (Figs. 1 and 2). The Zwillingsgletscher accumulation zone is located to the southeast of our study area between Lyskamm Peak and Pollux and Castor Peaks (Figs. 1B and 2A) near the Swiss-Italian border. In the

vicinity of our study area, the Zwillingsgletscher has a north-northwest flow direction, which changes to a mostly westward flow direction further downslope, well below the icefall.

The Zwillingsgletscher is part of a heterogeneous glacier system (i.e., it is not isolated like the Bas Glacier d'Arolla). For example, the Zwillingsgletscher is a narrow lobe with well-defined wave ogives, whereas the immediately adjacent Grenzgletscher is broad and more complex with no easily discernible ogives or other periodic topographic pattern. Unlike the Grenzgletscher (Eisen et al., 2009), no subsurface temperature data are available for the Zwillingsgletscher. Our study area consists of a 2.4-km length of the Zwillingsgletscher, in addition to separate surveys on the Grenzgletscher (Fig. 1).

METHODOLOGY

We used a Geophysical Survey Systems, Inc. (GSSI) 200-MHz antenna unit with two filter settings, 5–300 MHz (low-frequency version) and 50–600 MHz (high-frequency version), matching long and short record lengths, respectively (see following). The choices of antenna and field filters were guided by testing during the first two field seasons. Data were acquired during July 2009 (bare ice conditions with some surface water); May 2010 (averaging 0.73 m of snow cover along the survey profiles); and July 2011 (conditions similar to July 2009). All 2-D radar profiles were collected in continuous mode. The low-frequency profiles contain ~13.1 traces/m, with a sample rate of ~0.732 ns and a 1500 ns time range. The high-frequency profiles have ~39.4 traces/m, with a sample rate of ~0.244 ns and a 500 ns time range. During the surveys, we endeavored to keep the antenna level along the glacier surface, so that a correction for antenna tilting (directivity) was deemed unnecessary.

We recorded data along two approximately parallel transects on the Zwillingsgletscher (profiles Z1 and Z2, eastern and western profiles, respectively), each several hundred meters long and oriented parallel to glacial flow and perpendicular to the ogives, and along several cross transects, parallel to ogive strike, and a pseudo-3-D volume (Fig. 1). Two subparallel high- and low-frequency profiles were also acquired approximately along the flow direction of the Grenzgletscher, located 280–400 m east of the easternmost profiles on the Zwillingsgletscher. These profiles provided a “control” set of observations over an adjacent glacier that has no obvious ogives (profile G1, Fig. 1).

In July 2011, we conducted a grid survey in one area of ogives where the topographic variation and the subsurface radar scattering pattern

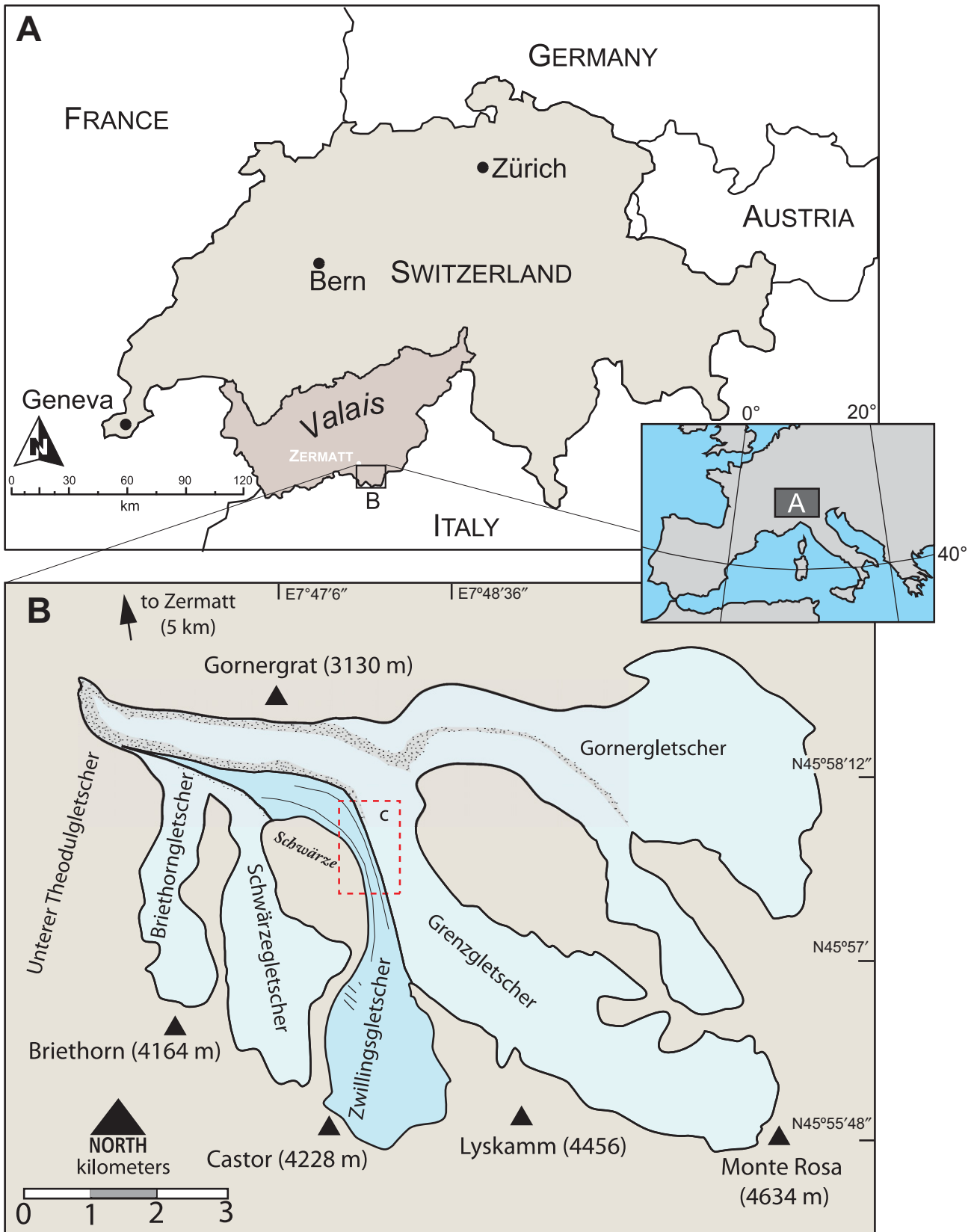


Figure 1 (on this and following two pages). (A) General location of the study area. (B) Outline of the Gorner glacier (Gornergletscher) system in Canton Valais, Switzerland (orange rectangle with “c” is map in Fig. 1C). The mountainous area labeled as Schwärze is also labeled in subsequent figures for reference.

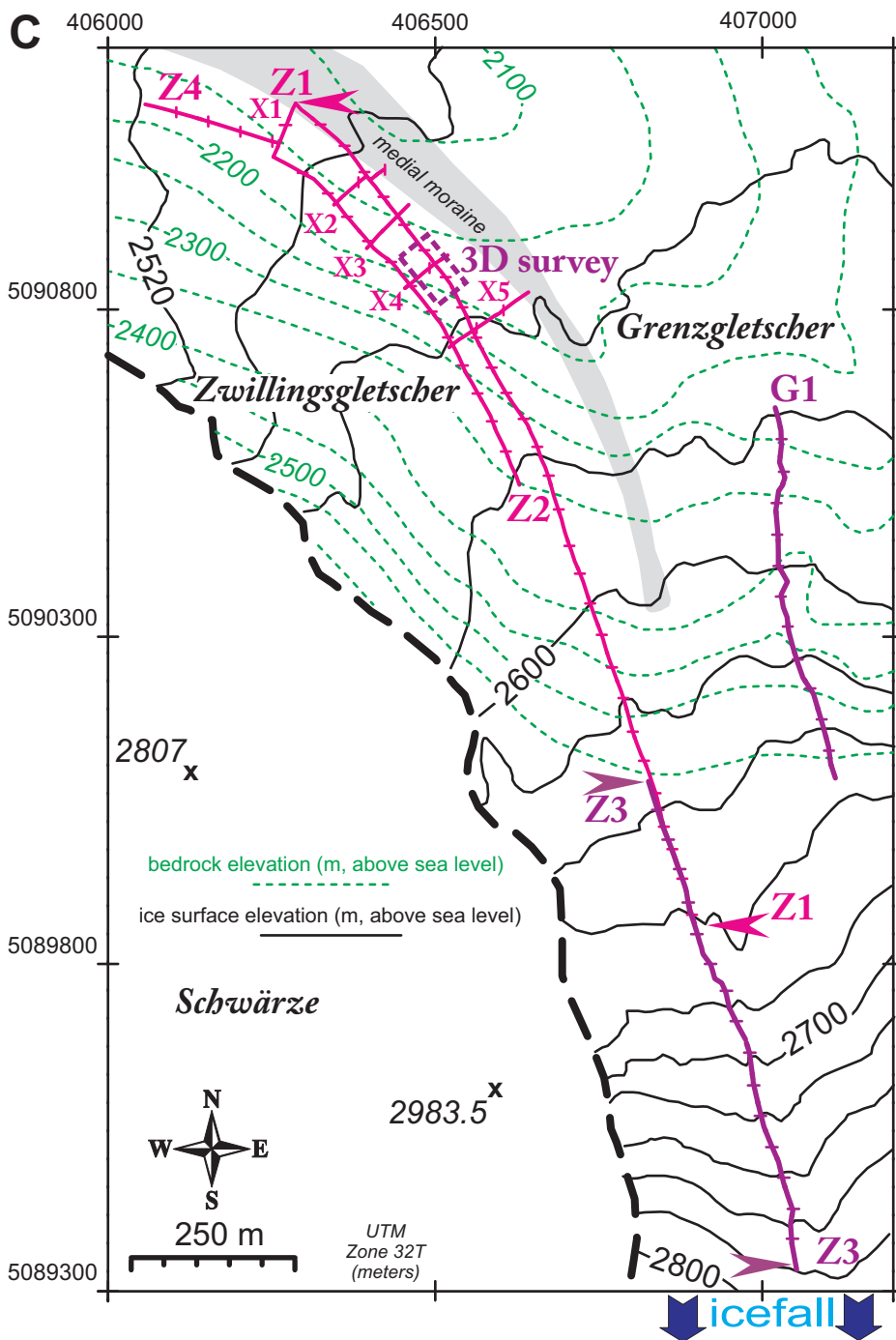


Figure 1 (continued). (C) Detailed map of study area (base map modified from Eisen et al., 2009) showing ground-penetrating radar (GPR) surveys collected for this study in 2009–2011. Note that the relationship between our surveys and features depicted on the base map are approximate due to glacial movement. Pink lines indicate radar surveys collected in May 2010; purple lines in July 2011. Tick marks on profile lines represent 50 m intervals (beginning of profile is always on the north or west). The icefall is just south of the map. The equilibrium line altitude is located much further to the south at ~3100 m above sea level. On this and subsequent maps, the vertical and horizontal axes are northing and easting (meters, UTM), respectively.

are complex (i.e., all variations are relatively short wavelength) (Fig. 1). The ice surface was free of snow, but it included some meltwater streams. We acquired 19 profiles (high-frequency acquisition filters, 750 ns record length, ~22 traces/m, sample rate ~0.366 ns) spaced 2–4 m apart (i.e., elevation grid was not perfectly regular), and covered an area of 90 m along the flow direction by 54.9 m across the glacier. This grid allowed us to re-bin the amplitudes in order to produce vertical views in any direction. Horizontal depth slices through the volume were generated by binning the data into a 3-D grid and then interpolating the data over a narrow depth range. Volume rendering was also performed (e.g., Kadlec et al., 2010) by reducing the general gain of the volume so as to accentuate only the highest amplitudes.

Our profiles were corrected for elevation, surveyed with an accuracy of a few centimeters. We used exponential gain compensation, corrected the data onset to zero time, applied background removal (mainly for direct arrivals), weighted 9-trace mixing to suppress clutter from surface water or man-made snow depressions, and applied constant-velocity migration and time-to-depth conversion. We translated the time range to depth using a wave speed of 0.16 m/ns, corresponding to a typical range in dielectric constant for ice of 3–4 (Milsom, 2003; Bradford and Harper, 2005). The recording times of 1500 ns and 500 ns for the 2-D profiles translate to depths of 120 m and 40 m, respectively. The solid ice velocity of 0.168 m/ns used by Eisen et al. (2009) for the adjacent Grenzgletscher differs by 5% from our value (we used a “standard” value, since the value from the Grenzgletscher is not necessarily expected to be identical to that of the Zwillingsgletscher). We display our profiles as reflection strength (e.g., White, 1991) in colorized amplitude formats (migrated or unmigrated) (Fig. 4). The low-frequency profiles were less susceptible to scattering (or guided wave development) or radar “ring-down” from meltwater streams (Radzevicius et al., 2000), relative to the high-frequency versions.

RESULTS

Two-Dimensional Surveys

Initial experimental ground-penetrating radar profiling on the Zwillingsgletscher in 2009 revealed a prominent scattering pattern in the upper 50 m of the ice (McBride et al., 2010), which led to further field seasons focusing on understanding this pattern. The first-order observation is an upper zone of low scattering (i.e., mostly nonreflective or “transparent”) that overlies a strongly scattering layer with an onset of

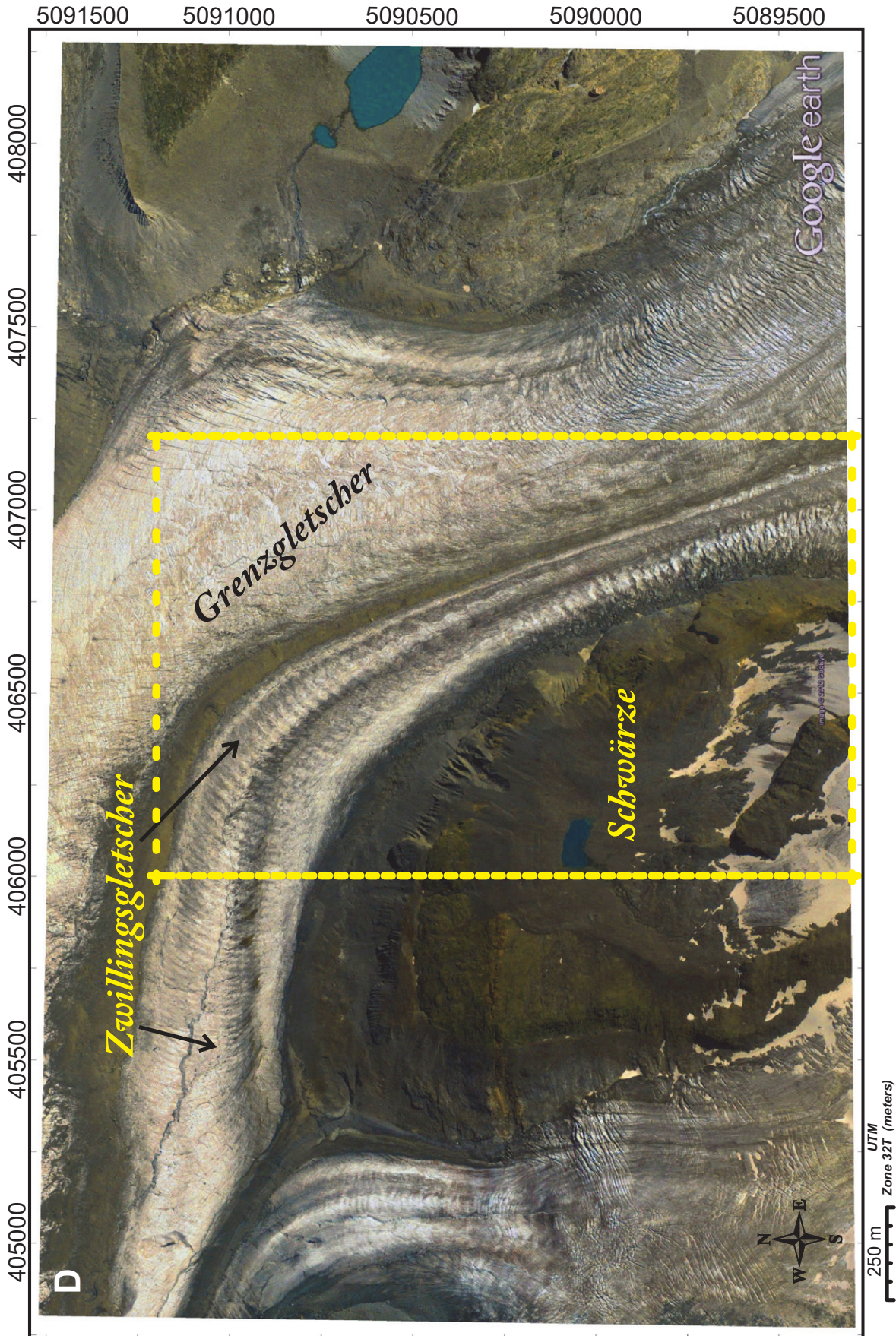


Figure 1 (continued). (D) Satellite image of a portion of the Gornergletscher system centered on the Zwillingsgletscher, dated October 2009 (aerial image from Google Earth Pro-license to Thomas H. Morris). Ogives are visible as a ribbed pattern traversing the Zwillingsgletscher. Dashed yellow rectangle corresponds to area of part C. Note that, because the glacial environment is dynamic, relationships on this image will not exactly match those of our maps or profiles.

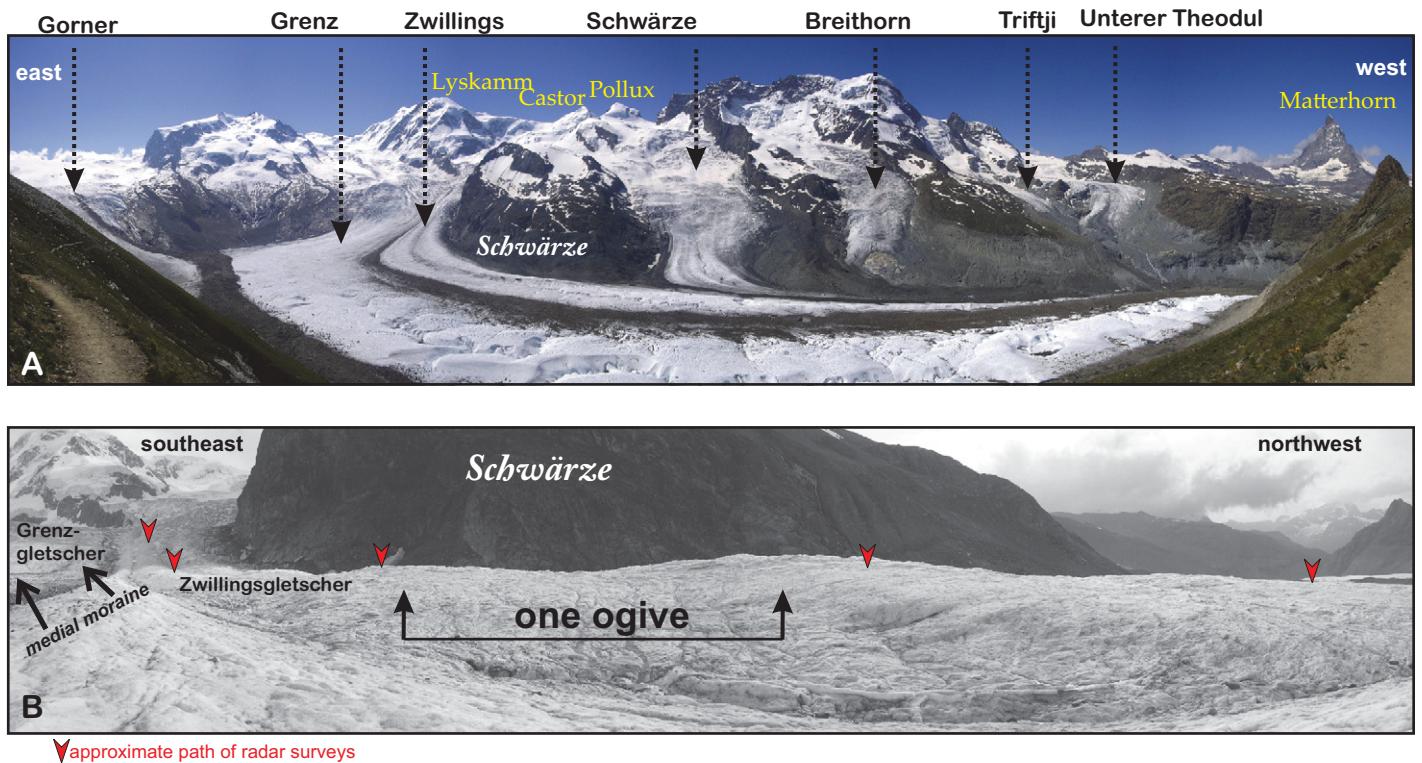


Figure 2. (A) Gornergletscher system in a panoramic photograph taken from the northern rim of the glacial valley (Fig. 1) looking south toward the Italian-Swiss border. Distance between Lyskamm and Matterhorn is about 15 km. (B) Panoramic photograph of the Zwillingssgletscher area of this study. Red arrows indicate the general line of our radar surveys. Photographs by Adam P. McKean.

5–20 m below the ice surface (Figs. 4 and 5). The thickness of the transparent zone decreases down glacier (cf. Figs. 5A and 6). Results from field seasons with snow cover and bare ice are virtually identical, the only difference being the effect on the high-frequency profiles of flowing meltwater streams that could not be avoided (July 2009 and 2011). Such streams caused strong low-apparent-velocity (i.e., steeply “dipping”) noise from scattering, or guided waves produced by the high-impedance water-ice contacts. This effect was mostly nonexistent for the snow-covered glacier, although spurious horizontal arrivals appear to be caused occasionally by the power/data cable being dragged through the snow.

The high-frequency and low-frequency versions showed identical behavior for the onset time of scattering (or strong reflectivity) (Fig. 5). This onset is expressed as a “sinusoidal” or undulating pattern for which wavelength increases up glacier (to the southeast). Goodsell et al. (2002, p. 287) described a similar pattern from the Bas Glacier d’Arolla as “alternating reflection-rich and reflection-poor zones,” but did not describe a change in wavelength of this pattern. Moving down glacier (to the northwest) along profile Z1 (Fig. 5A), the wavelength of this pattern shortens drastically

as the profile obliquely approaches the medial moraine that divides the Zwillingssgletscher from the Grenz-gletscher. As profile Z1 begins to abut the moraine, the well-patterned scattering onset gradually loses its clear periodic character, becoming more of a uniform-depth onset with no coherent shape. A short, parallel profile (Z2, Fig. 5B) located near the center of the Zwillingssgletscher shows a similar pattern of increasing wavelength up glacier, but without the drastically shortened wavelength down glacier as seen nearer the moraine on profile Z1. The progressive increase in the wavelength of the scattering pattern continues up glacier beyond the southeastern end of profile Z1 closer to the icefall zone, as shown on short profiles acquired July 2011 in between major transverse crevasses (i.e., crevasses trending perpendicular to ice flow direction) (Fig. 6). Collecting data further up glacier was not possible due to safety concerns and the abrupt increase in the roughness of the ice surface and crevasses (Fig. 3B). On the down-glacier end of the Zwillingssgletscher study area, the scattering pattern appears to deteriorate to the northwest of profile Z2 (i.e., on profile Z4, not shown).

The peaks of the periodic pattern are well expressed as either distinct diffractions or short

planar reflection segments; the latter appear after the sections have been migrated, which collapses diffraction hyperbolae into “point” reflectors using the velocity of 0.16 m/ns (Fig. 4; McBride et al., 2010). We investigated modeling of hyperbolae to obtain velocity structure but found the variation (likely to be influenced by out-of-plane effects) to be too great. The polarity of the reflectivity is usually negative (Fig. 4), suggesting a material property change from higher to lower velocity (e.g., as would be expected for solid ice transitioning to pockets of liquid water [or rock] that scatter the radar signal); however, this behavior varies. The peak areas are laterally separated from reflection-poor areas. This effect is more obvious as wavelength increases up glacier. The reflection-poor areas are not as well defined as the reflective peak areas, making the observation of a “sinusoid” pattern for the onset of scattering largely dependent on the peak areas. The wavelength of the periodic scattering varies from ~155 m up glacier to ~30 m down glacier. The amplitude of the periodic scattering pattern is much greater than that of the surface ogive topographic pattern. Although the onset of scattering is relatively well defined, the base is not, and may be dependent on frequency and attenuation.

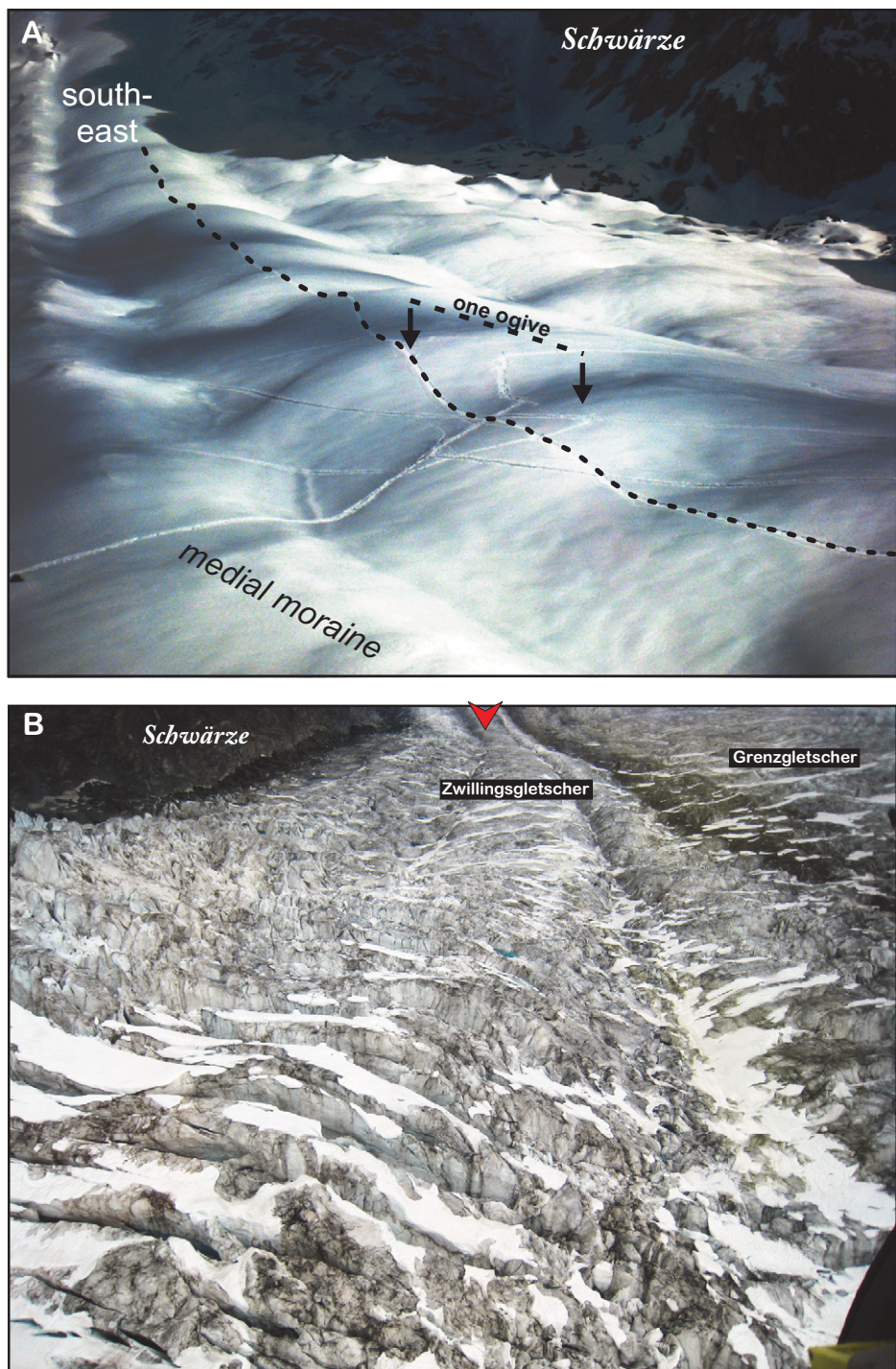


Figure 3. (A) Aerial photograph (artificial shading applied to accentuate ogive slopes; no banding in the snow was observed) of the Zwillingsgletscher with less than 1 m of snow cover (May 2010) looking to the southeast. Ogive pattern is expressed by undulating surface. Longitudinal path in the snow shows path of Z1 profile (Fig. 5A). Photograph by John H. McBride, taken from helicopter. (B) Aerial photograph of crevasses within the icefall zone of the Zwillingsgletscher, looking down glacier, to the northwest. Vertical orange arrow shows approximate up-glacier limit of our ground-penetrating radar surveys. Photograph by David G. Tingey, taken from helicopter.

Five cross profiles (perpendicular to the direction of glacial flow) were also acquired across the Zwillingsgletscher and connecting the two longitudinal profiles Z1 and Z2 (Fig. 1). The cross lines allowed us to determine if the periodic pattern was unique to the longitudinal profiles and was thus related to glacial flow processes. The cross profiles significantly vary, but without the clear pattern of alternating strong and absent scattering on the longitudinal profiles (Fig. 7A). Instead, weaker scattering generally follows topographic slope at 5–15 m below the ice surface, interrupted in places by patches of strong reflectivity (including diffractions) and by numerous bright planar reflectors that consistently dip steeply to the southwest (in the plane of the cross profile). Although cross-line control is limited, these planar reflectors seem to correlate with nearly flat (or gently dipping, usually down glacier) planar reflectors on intersecting northwest-oriented glacier-parallel profiles and define west-to-southwest-dipping surfaces in three dimensions (Fig. 7B). The planar reflectors frequently emerge in shingled sets (e.g., spaced ~5–15 m apart) with a maximum apparent dip of ~25° (e.g., Fig. 7A) and do not reach the ice surface (or at least are not imaged near the surface). These reflectors are commonly also associated with, and interrupt, areas of increased scattering, but they may also form “bridges” across the reflection-poor zones. Two long profiles obtained over the adjacent Grenzgletscher (G1 and G2, Fig. 1), which has no noticeable ogive pattern (topographic or banded), mostly show a uniformly nondescript and nonreflective character (Fig. 8). Profiles acquired at 40 MHz for the same area by Eisen et al. (2009) likewise show a broad region of “low backscatter” down to ~170 m depth (their profile P05–2).

Three-Dimensional Survey

The 3-D volume survey shows a well-developed periodic scattering with three peaks separated by areas of reduced scattering (Figs. 9 and 10). Another feature is a set of two or three strong planar reflectors that trend with topographic slope (in the plane of the longitudinal sections) and appear to cut the periodic scattering pattern (Figs. 9 and 11). As observed on the transverse 2-D profiles, these planar reflectors do not reach the ice surface and have a west-southwest dip direction (Fig. 9). Although periodic scattering persists across the volume, this pattern becomes more coherent closer to the center of the glacial lobe (to the southwest) (Fig. 10). The character of the scattering pattern as well as of the planar reflectors is similar to that found on nearby 2-D regional profiles (Figs. 1C and 5). Horizontal depth slices (Figs. 10 and 11) also show that the

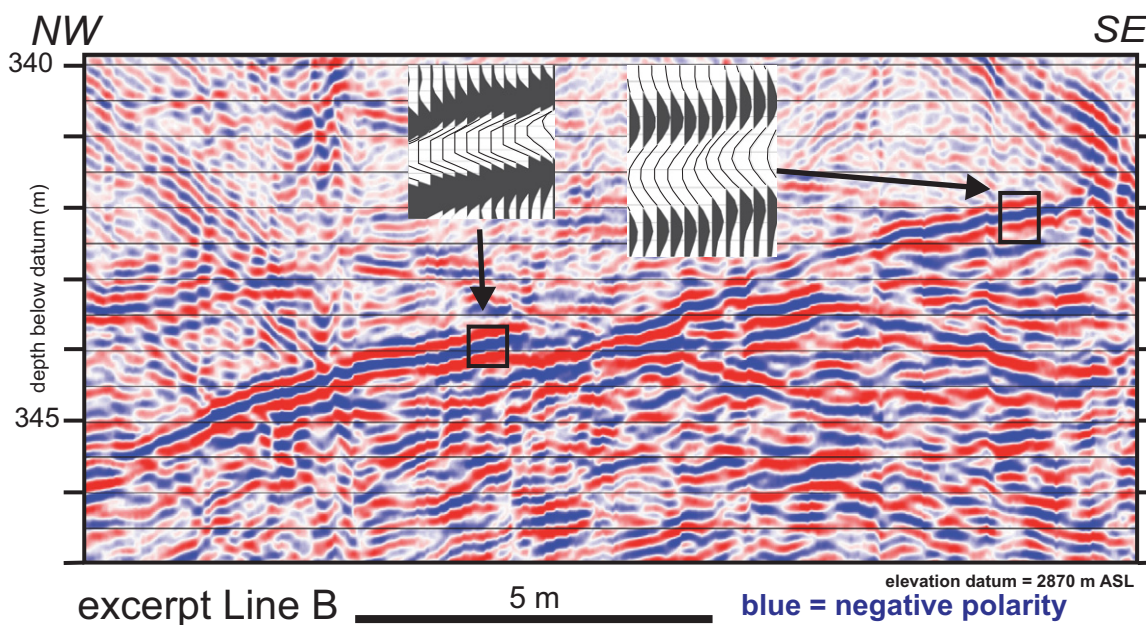


Figure 4. Portion of the unmigrated ground-penetrating radar profile from southern part of line B from pseudo-three-dimensional volume at the onset of scattering shown as a color amplitude section with no trace mixing. Two small wiggle-trace displays show negative polarity of the energy (red is positive polarity; blue is negative). ASL—above sea level.

scattering pattern is strongest to the southwest, moving away from the medial moraine, and is composed of three prominent scattering peaks.

In order to observe relationships between the periodic scattering and the planar reflectors, we rendered the amplitudes in the 3-D volume to emphasize only the high values. Perspective views of this rendering (Fig. 12) and video of the 3-D volume (see Animation 1) reveal that the apparently subhorizontal planar reflectors in the longitudinal profiles actually represent steeply southwest-dipping (true dip) reflectors that are prominent nearer the medial moraine and appear to dip into and beneath the three scattering peaks to the southwest. The true dip of these reflectors is close to that of the dipping reflectors on the single transverse profiles (Fig. 7A). While these planar reflectors are not imaged near the surface, our July 2009 field observations indicate that the orientation of secondary ice foliation intersecting the ice surface mimics the true dip of the subsurface reflectors in regions close to the medial moraine.

DISCUSSION

Geometric Relation of Radar Scattering to Ice Surface

The chief observation from our study is a transparent 5–20-m-thick layer of glacial ice underlain by a layer with periodic scattering

zones. This pattern is independent of season (spring vs. summer) and snow cover (snow vs. bare ice). The periodicity decreases in wavelength in the direction of glacier flow. Note that, although troughs in the radar scattering are not well defined, the peaks are (Fig. 4). Moving up glacier, convex-upward pods of high scattering are increasingly separated from areas of reduced or absent scattering (Fig. 5A). The periodicity of the scattering onset mimics the topography of the wave ogives, although the scattering pattern and topographic highs and lows are not necessarily in phase (the amplitude of the wave ogives is much less than that of the scattering) (Fig. 5A). Along profiles Z1 and Z2, we compared ice topography with the depth of the scattering onset (Fig. 13) in order to quantitatively relate glacial surface characteristics to the subsurface scattering. Gradients of the surfaces were used to accentuate variations. The onset of subsurface scattering was first interpreted from the profile and digitized and also expressed as the isochore between ice surface and the interpreted scattering onset (i.e., the vertical thickness of the upper transparent zone) (Fig. 13). Next, the gradient of this surface was computed and compared with the gradient of glacial topography, along with the second derivative of glacial topography. The results show a fairly good correspondence between the periodicity of the glacial surface and that of the strong scattering onset (Fig. 13). A match between the up-glacier progression from short to long wavelengths for the ice

topography and the subsurface scattering onset is also observed, although the longer profile Z1 shows this relationship more clearly. From Figure 13, we can see how the distance between the peaks and troughs in the gradient of the scattering surface progressively collapses moving down glacier. In particular, starting on the southeastern end of profile Z1, the crests of the ogives become increasingly out of phase with the peaks of the scattering onset further down the glacier. The overall correspondence between scattering and the ogives points to a possible genetic link between the glacial processes giving rise to the scattering onset and the development of the ogive-dominated surface.

A one-to-one correspondence between the subsurface pattern and the glacier surface is not expected because each is altered over time by different processes. Ablation would alter the surface structure, while compression from ice flow would alter both the surface and subsurface structure. The down-glacier decrease in the thickness of the transparent zone, which likely is an effect of increased total ablation in older ice, follows the pattern of ogive topographic crests and scattering peaks, becoming increasingly out of phase down glacier. The phase shift also tends to occur where there is a break in topographic slope (Fig. 5). Surface slope is steeper in the up-glacier portion of the radar profile and is shallower down glacier. Since ice flow from internal ice deformation (ignoring basal sliding) is, on average, proportional to surface slope to

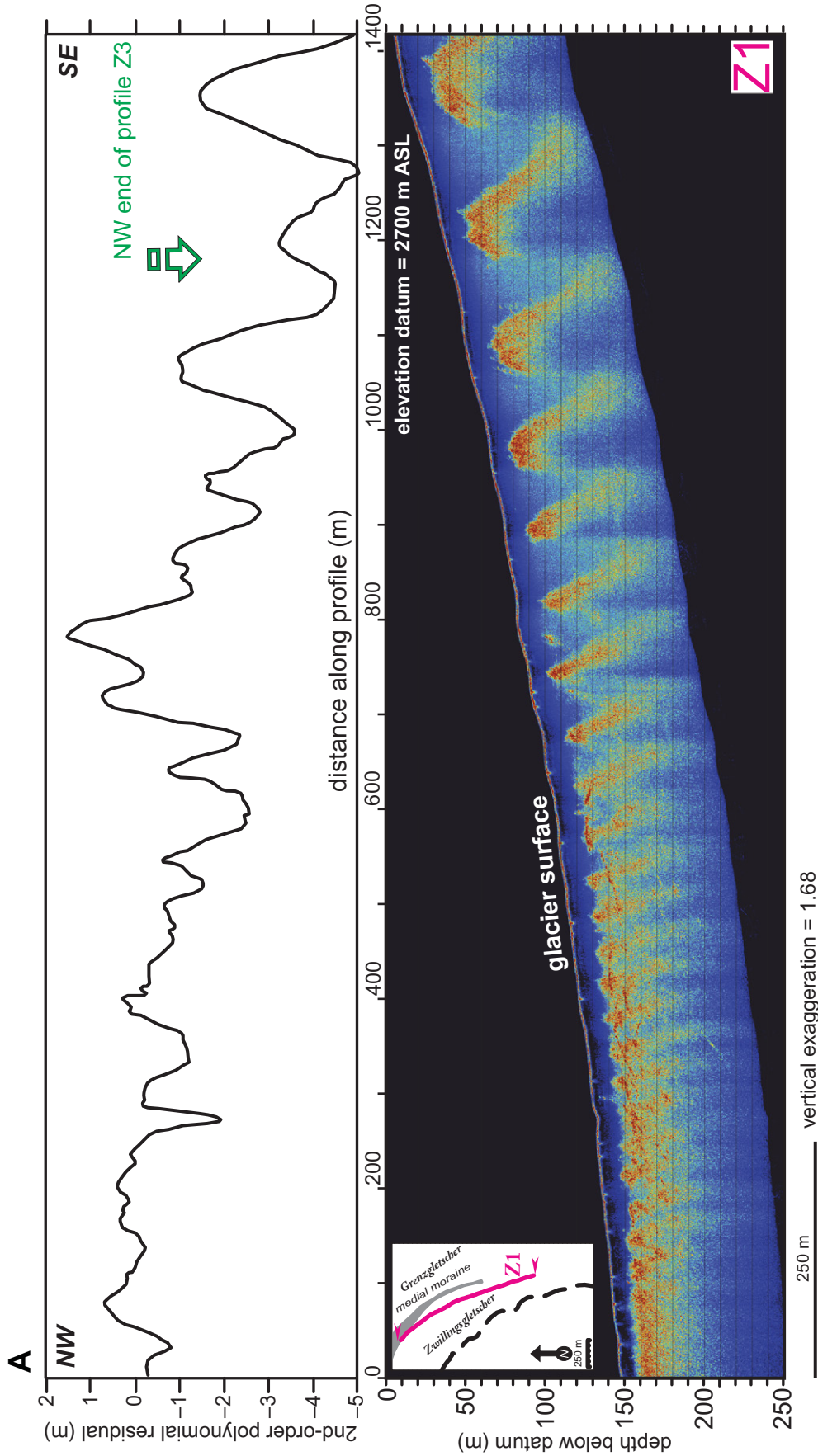


Figure 5 (on this and following page). (A) Profile Z1, collected May 2010 (see text for data processing description) (low-frequency version), migrated and processed as reflection strength (hot colors indicate high strength, cold low strength [e.g., see White, 1991; Sheriff and Geldart, 1995]; see text for details). Upper part of figure shows residual elevation. Note that the southeastern part of this profile overlaps with profile Z3 (Fig. 6). See inset map and Figure 1C for locations for this and subsequent profiles. (B) As in A, but for profile Z2, collected May 2010. This profile was located along the southwestern, downslope margin of the wave ogives. ASL—above sea level.

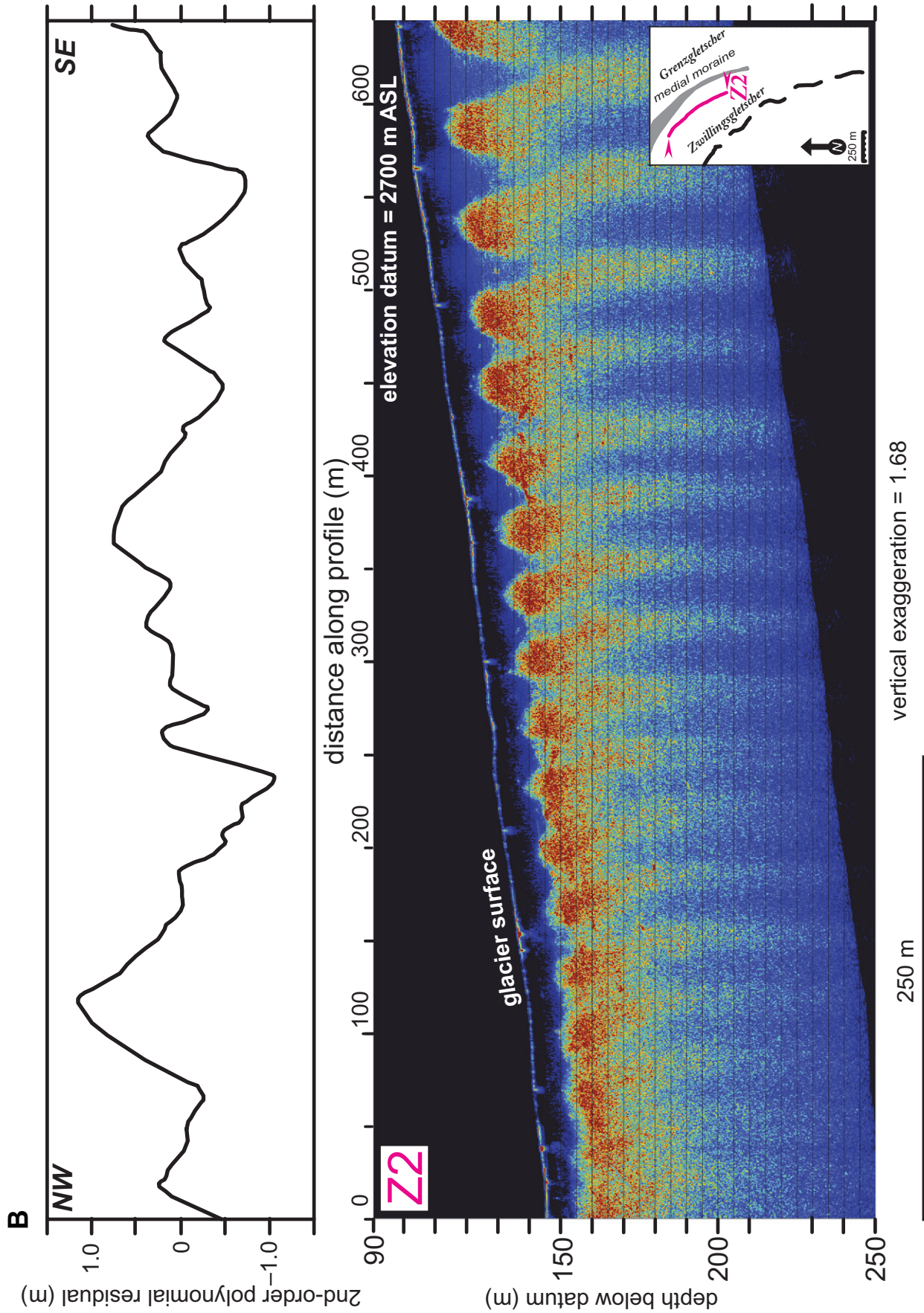


Figure 5 (continued), (B) As in A, but for profile Z2, collected May 2010. This profile was located along the southwestern, downslope margin of the wave ogives. ASL—above sea level.

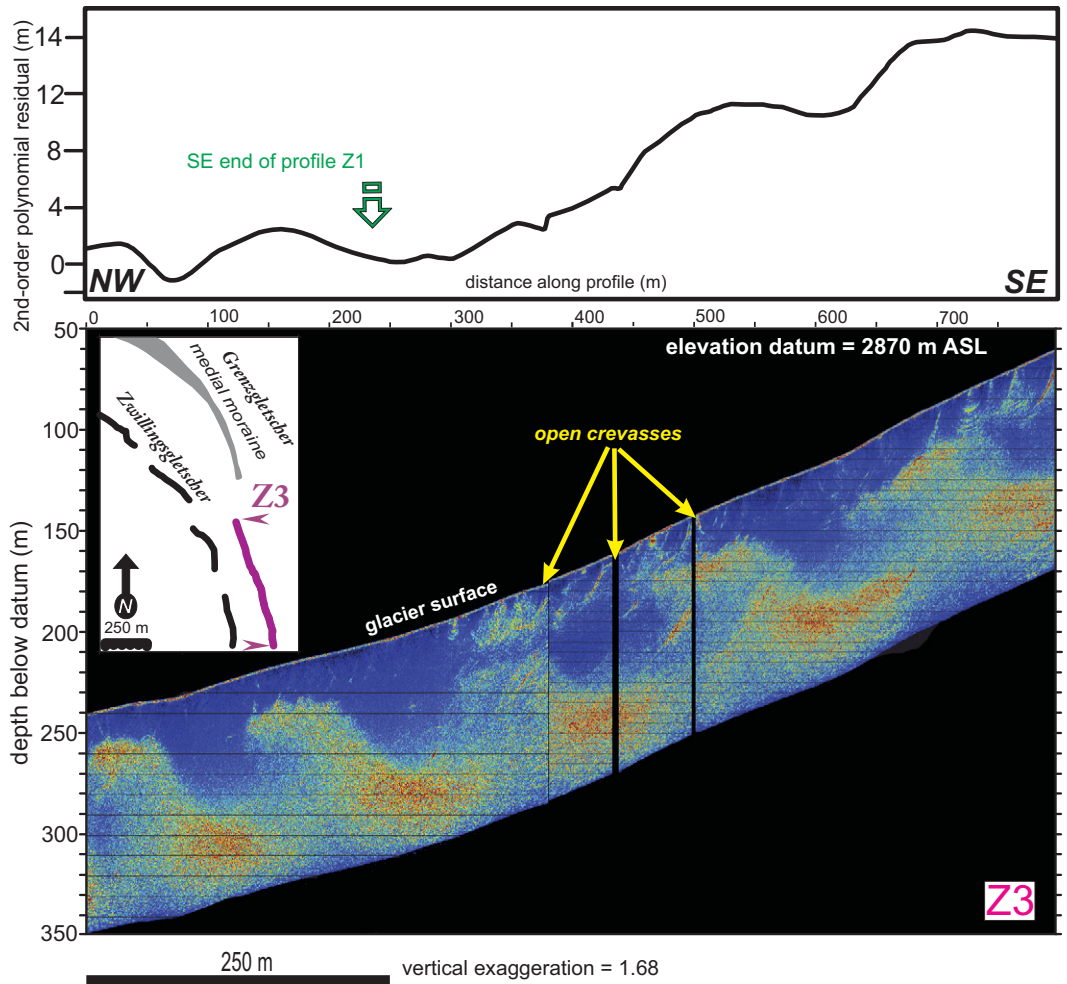


Figure 6. Profile Z3, collected July 2011, from up-glacier position shown in Fig. 1C (see text for details). Note that the northwestern part of this profile overlaps with profile Z1 (Fig. 5). ASL—above sea level.

the third power (Cuffey and Paterson, 2010), compression will increasingly dominate ice flow down glacier, where the scattering zones become more compacted. Further, the down-glacier compression of ogives and radar scattering along our profiles is likely because ice is forced against the medial moraine and is located just up glacier of the confluence with Schwärzeglletscher. Based on both direct surveying and the change in wavelength of the ogives, the average velocity in the upper portion of the study area is $\sim 155 \text{ m yr}^{-1}$, and it decelerates to $\sim 75 \text{ m yr}^{-1}$ in the down-glacier portion of the study area. This indicates a significant amount of deceleration over a distance of $\sim 1.5 \text{ km}$ and results in an average longitudinal strain rate approximately -0.027 yr^{-1} . Thus, the combination of surface ablation and subsurface deformation would alter the phase relationship between ogives and radar scattering over time. In addition, the radar view likely does not follow the exact flow line of the glacier. The steep topography, location of surface meltwater, and the extent of the medial moraine made it difficult

to ensure that the radar profile exactly followed the gradient in ice thickness. Thus, the reflectors may also become increasingly out of phase with the surface topography if the radar view moves progressively off the flow line down glacier.

Near the northwestern end of our study area (Fig. 1), the gentle undulating topography on the Zwillingsgletscher is less obvious than it is further up glacier. So as to compare the topographic signal of the 3-D radar volume with the scattering pattern, a horizontal gradient was computed on the ice topography (Figs. 11A and 11B), analogous to computing the slope on the 2-D topographic profiles. We next interpreted an interval between the ice surface and the onset of scattering (i.e., the isochore of the upper transparent zone) (Fig. 11C). Comparison of the resultant maps (Fig. 11) shows that the three scattering peaks approximately match the three zones of anomalous ice topography expressed as negative-gradient (Fig. 11B) and residual (Fig. 11C) values. The three-part pattern expressed by the gradient map (Fig. 11B) is also shown by a residual elevation map (Fig.

11C). The correspondence is best expressed on the southwestern half of the volume where the three-part scattering pattern is best developed; however, the correspondence weakens closer to the medial moraine (i.e., to the northeast), possibly due to ablation of the ice surface and/or interference with the moraine.

Interpreted Deformation Features

The progressive decrease in the wavelength of both wave ogives and the correlated radar scattering pattern suggests a strain effect whereby the glacial ice is longitudinally compressed. We suggest this is the result of the confluence of the Zwillingsgletscher with the Schwärzeglletscher and the Grenzletscher, and the decrease in surface slope and associated decrease in ice flow down glacier, which together progressively inhibit flow further down glacier. One might expect this strain to be expressed in other subsurface structures. Although our profiles reveal abundant planar reflectors, they are not necessarily oriented in

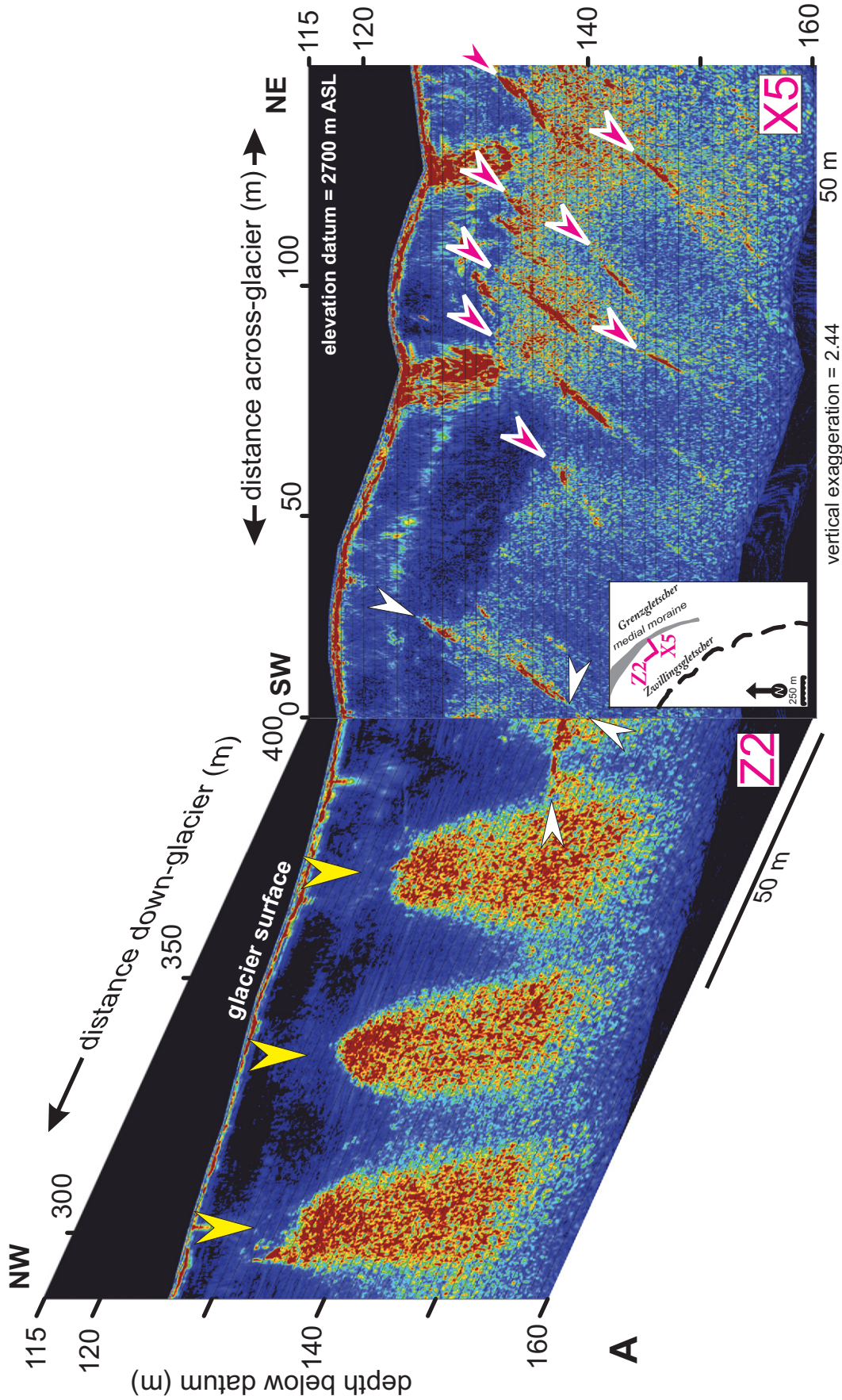


Figure 7 (on this and following page). (A) Along-dip (left) and along-strike (right) profiles showing correlation between steeply dipping reflectors on the transverse profile (X5) and gently dipping reflectors on the longitudinal (Z2, excerpt; perspective view) profile. Yellow arrows locate strongly scattering zones following the ogives. Red arrows indicate cluster of planar dipping reflectors typically observed on the transverse ground-penetrating radar profiles (see Fig. 1 for location of these profiles). White arrows show reflector mapped in B. Note that profile X5 obliquely cuts the flank of an ogive-related scattering area. This figure shows the interpreted fracture pattern. The data are processed and displayed as in Figure 5, but with a greater vertical exaggeration.

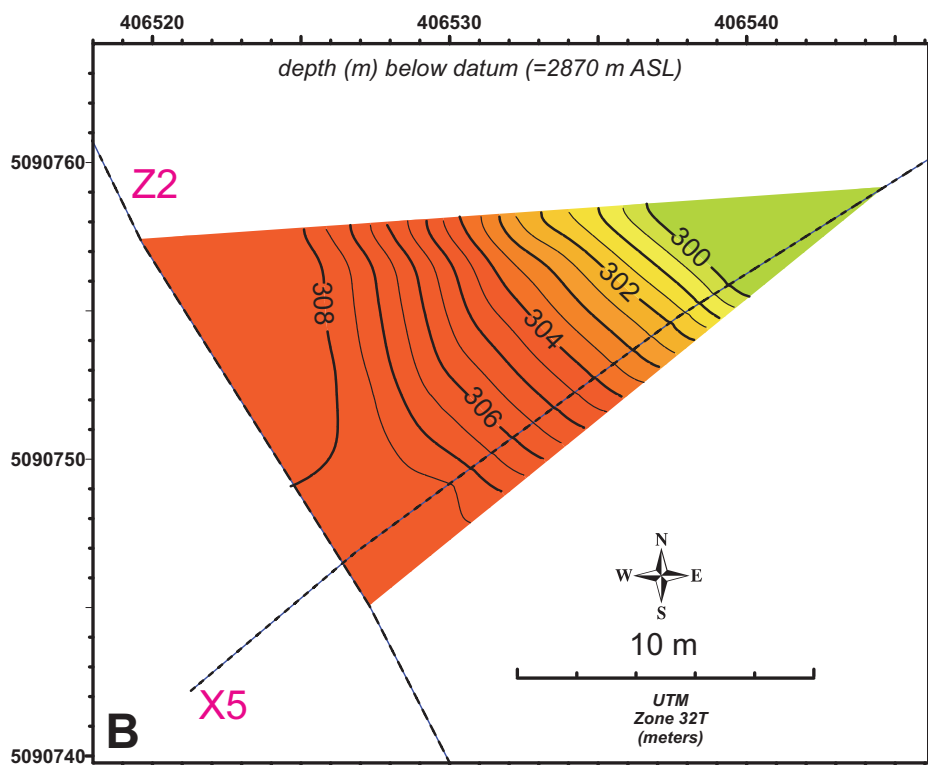


Figure 7 (continued). (B) Simplified contour map of the dipping reflector marked by the white arrows in A, and showing the north-northwest strike direction of planar reflectors that characterize the Zwillingsgletscher. ASL—above sea level.

the expected direction of dominant strain. These reflectors are observed on both regional longitudinal (Fig. 5) and transverse (Fig. 7A) profiles as well as within the pseudo-3-D volume (Fig. 12). From intersecting 2-D profiles and the 3-D volume, planar reflectors have a west-southwest dip direction (Figs. 7 and 12), which is neither exactly parallel nor perpendicular to glacial flow, although the north-northwest strike of the dipping reflectors in the 3-D volume is similar to the trend of the bedrock valley underlying the Zwillingsgletscher (cf. Figs. 1 and 11B). This may suggest a relationship between the confluence direction and the combination of shear and strain that produces the planar reflectors.

Planar or arcuate (in 2-D profiles) reflectors in glaciers have been interpreted as shear deformation features. For example, Appleby et al. (2010) interpreted them as thrusts formed by longitudinal compression below an icefall. They cited two cases where low-angle reflectors dipped up glacier (i.e., opposite to the glacier flow) and intersected an undulating ice surface in a manner that could be interpreted as thrust faults bringing deeper ice nearer the surface in the hanging wall of the fault (i.e., the fault verges down glacier [see also Goodsell et al., 2002]). Crevasse traces may also provide zones of preexisting weakness

(e.g., as shear planes) that can be reactivated as thrust faults by compressive stresses (Nye, 1951; Goodsell et al., 2002, 2005; Appleby et al., 2010). Bamber (1987) explained such reflectors to be water, which locally would imply temperate ice. Irvine-Fynn et al. (2011) suggested that thrust faults could provide “hydraulically transmissive sites.” Harper et al. (2010) mapped radar reflectors as water-filled fractures. As for our case, these water-filled fractures did not propagate into the near-surface region of the ice. Fountain et al. (2005) hypothesized that englacial fractures may indeed be the primary way in which water moves through temperate glaciers.

If such planar features could be visualized in a 3-D volume, they might be expected to have a dip direction that is perpendicular to the strike of the topographic undulations (i.e., parallel to the flow direction). Our mapping shows that the planar surfaces dip west-southwest (striking north-northwest), which is not parallel to the locally northwest direction of glacial flow and the northeast-southwest strike of the subsurface scattering pattern. The dipping surfaces do not appear to accommodate deformation of the ogive-shaped ice surface or the scattering pattern (at least in a simple way), although these surfaces cut below and through the scattering

pattern. We suggest that the planar surfaces are either partially healed crevasses with remnants of liquid water or shear planes or fractures that are also filled with water. In either case, the planar structures do not support a thrust fault formation for the ogives (Posamentier, 1978).

Comparison of Radar Scattering from Other Glaciers

The radar patterns on the Zwillingsgletscher are considerably different from those observed by Eisen et al. (2009) with lower-frequency antennas on the adjacent Grenzgletscher (Fig. 1). An onset of scattering was observed there, but it is about one order of magnitude deeper than we observed on the Zwillingsgletscher. In particular, Eisen et al. (2009) detected a several-hundred-meter-wide layer of ice with a maximum thickness of 381 m (measured from a borehole). This layer included an upper layer of cold ice, partially expressed on radar profiles as a transparent (i.e., low “backscatter”) zone, up to 286 m below the surface. Below this depth (the cold-temperature transition surface), temperatures increased toward the pressure melting point of ice, and radar profiles were dominated by scattering (i.e., the scattering onset is systematically shallower than the cold-temperature transition surface). These lower-frequency surveys detected no radar structure that could be related to wave or band ogives. Consistent with their results, our reconnaissance profiles over the Grenzgletscher (G1, Fig. 8) likewise show no scattering pattern like that observed on the Zwillingsgletscher.

On the other hand, our Zwillingsgletscher profiles are similar to those from the Bas Glacier d’Arolla shown by Goodsell et al. (2002), who interpreted the periodic pattern of high and low reflectivity as being related to the alternating foliation-rich dark and foliation-poor light ogive bands, respectively. Areas of pronounced scattering on the Bas Glacier d’Arolla were interpreted as “changes in ice properties across foliation boundaries” (Goodsell et al., 2002, p. 296). The more intensely foliated dark bands were interpreted to have trapped more fine debris, due to differential weathering, and to represent ice exhumed during rotation at the base of the icefall where ogive formation commences. Unlike the study of the Grenzgletscher (Eisen et al., 2009), or our Zwillingsgletscher observations, no association was drawn between zones of radar scattering and water-inclusion (or temperature) effects. We did not detect zones of debris-rich, foliated ice on the Zwillingsgletscher.

A rich body of literature is available, drawing associations between radar scattering and temperature, liquid water content, and/or rock

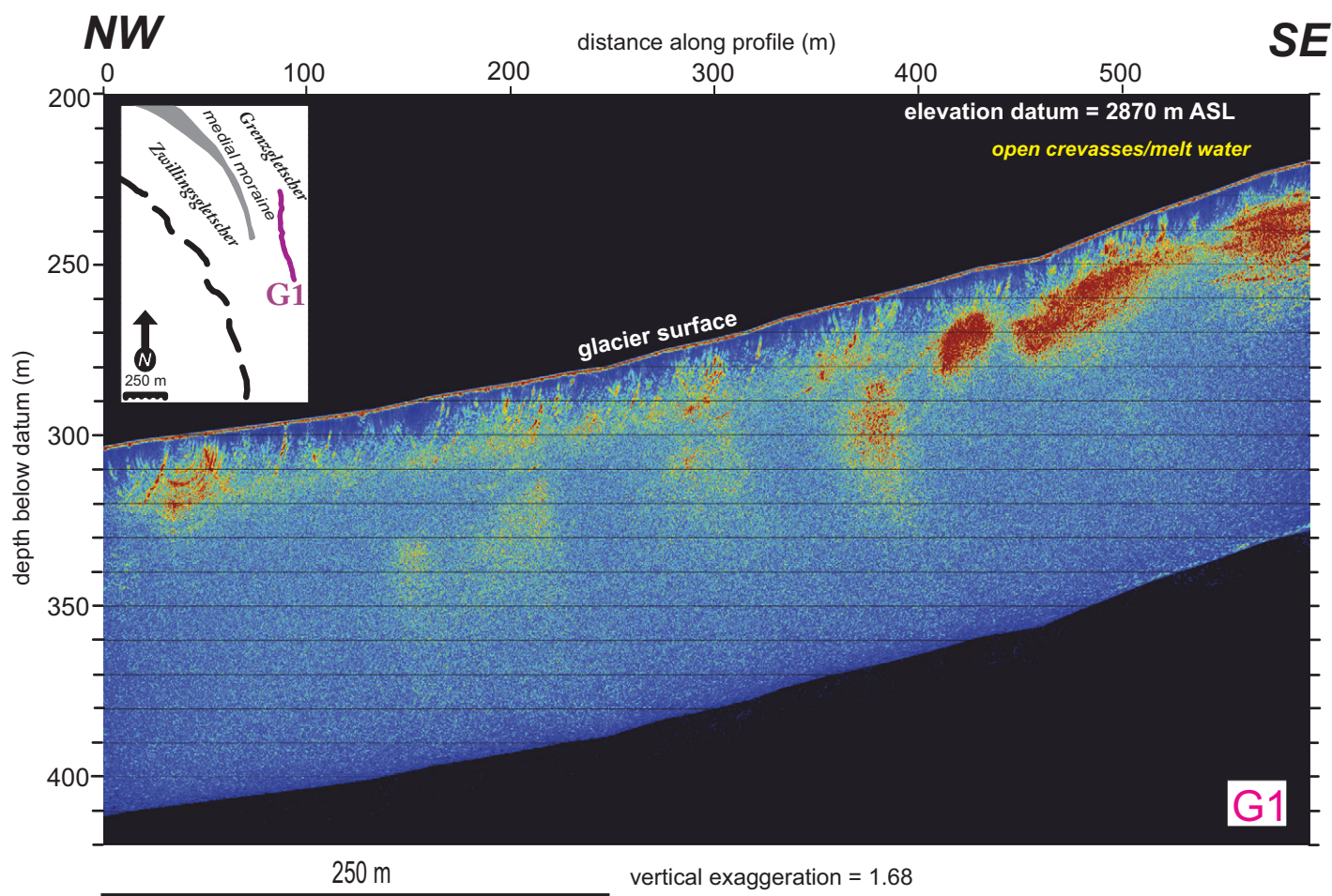


Figure 8. Profile G1 over the Grenzletscher (low-frequency version) in July 2011 showing lack of clear regular, periodic radar scattering pattern. Note that the profile ends to the southeast within a set of crevasses that trend subparallel to the profile and may be expressed as sideswipe on the profile. The data are processed and displayed as in Figure 5. ASL—above sea level.

debris (e.g., Bamber, 1987, 1988; Hamran et al., 1996; Moorman and Michel, 2000; Goodsell et al., 2002; Pettersson et al., 2003; Irvine-Fynn et al., 2006, 2011; Woodward and Burke, 2007; Bradford et al., 2009; Brown et al., 2009). However, associations between scattering and temperature have not consistently been reported. For example, temperate ice (i.e., “warm” ice, hosting liquid water) is frequently associated with intense radar scattering (e.g., Björnsson et al., 1996; Murray et al., 2007; Macheret et al., 2009; Bælum and Benn, 2011). Polythermal glaciers may show a correlated, two-layer temperature and reflectivity structure “indicated by a shift from a clear layer with few reflections to a more opaque and noisy layer with numerous small reflections” (Bælum and Benn, 2011, p. 146; Eisen et al., 2009). Alternatively, coincident temperature and radar measurements in other polythermal or temperate glaciers do not show such a correlation (Jania et al., 1996; Brown et al.,

2009). Although radar-transparent ice overlying a strongly scattering zone has been taken to indicate cold ice overlying temperate ice, Brown et al. (2009, p. 1497) cautioned that “spatially extensive radar-transparent layers normally used to identify cold ice in polythermal glaciers are present in some temperate glaciers,” based on observations from the Bench glacier, Alaska.

Provisional Hypothesis for the Origin of Radar Scattering within the Zwillingsletscher

Our ability to definitively interpret the origin of the scattering pattern within the Zwillingsletscher is limited by the absence of subsurface ice temperature measurements. We thus examine multiple explanations for the observed scattering pattern.

The shearing hypothesis is not entirely consistent with our observations from the Zwillings-

letscher for the following reasons. (1) We do not observe surfaces with a strike and dip that match the strike and dip of the wave ogive pattern and its correlated radar scattering pattern. (2) Debris-laden ice, which would have been uplifted from depth, is not observed in the troughs of the ogives. (3) The strong scattering is more consistent with water inclusions than with rock debris. The dielectric constant of glacial ice (3–4) is not drastically different from typical silicate-dominated rock fragments when compared with liquid water (e.g., compare dielectric constant of granite [with quartz (~4.5), feldspars (5.7–7), and micas (7–9)] with that of liquid water, which is ~88 at 0 °C [Steven A. Arcone, 2012, written commun.]). Further, abundant diffractors (Fig. 4) appearing at the base of the transparent zone may be explained by small (with respect to our radar wavelengths) water pockets that strongly scatter radar energy. Bamber’s (1988) theoretical model indicates

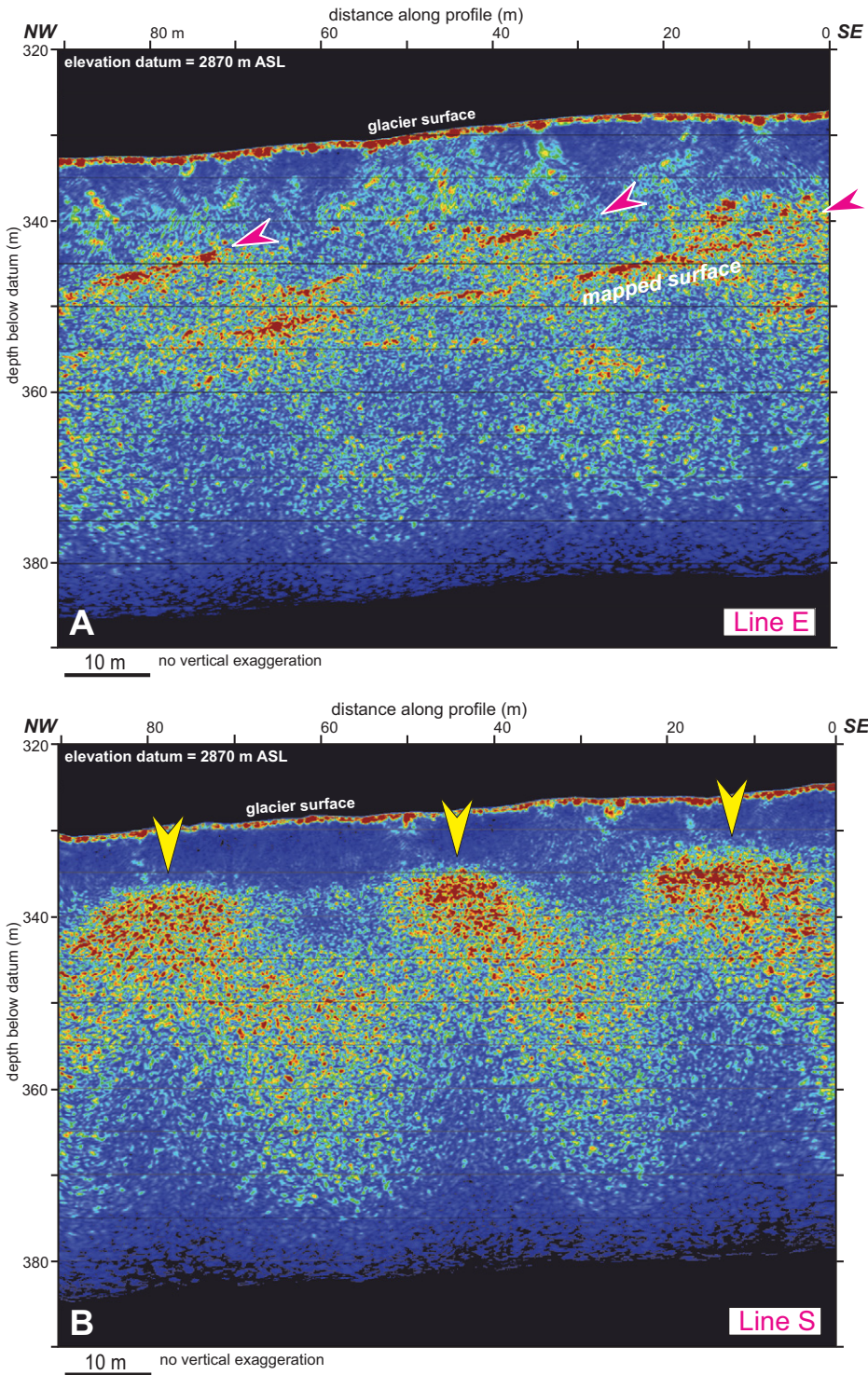


Figure 9. (A) Vertical profile view from pseudo-three-dimensional (3-D) volume showing planar reflector pattern (red arrows) that dominates the northeastern portion of the volume, nearer the medial moraine (see Figs. 1C and 10A for location). The reflector mapped in Figure 11 is noted. (B) Vertical profile view from pseudo-3-D volume showing periodic scattering pattern (yellow arrows), correlated with ogive development that dominates the southwestern portion of the volume, nearer Schwärze (see Figs. 1C, 10, and 11 for location). ASL—above sea level.

how a sub-meter-sized water inclusion can powerfully scatter electromagnetic radiation, compared to a planar reflector. (4) The periodic scattering in the Zwillingsgletscher, as well as the decay in the wavelength of the scattering down glacier both point to a phenomenon linked to summer versus winter (i.e., annual) variations. We note that the observations of a scattering onset of 5–20 m below the ice surface accord well with depths reported for temperature inversions correlated to the radar scattering onset elsewhere (Gusmeroli et al., 2010).

The seasonal variations in ice flow through the heavily crevassed icefall may give rise to thermal variations in that ice. We suggest that a polythermal distribution is set up seasonally at the icefall zone for the Zwillingsgletscher, as shown by the model in Figure 14. In the icefall zone, plentiful crevasses form with many orientations, depths, and extents. Surface meltwater drains into these crevasses throughout summer. Assuming that the crevasses can retain water (e.g., do not all extend to the glacier bed), the seasonal filling and subsequent freezing (and associated latent heat release) of water-filled crevasses could yield seasonal pockets of temperate ice during the fall and winter (Fig. 14). Importantly, laterally extensive crevasses would be efficient at homogenizing the ice temperature during the period of freezing and latent heat release. Such an annual variation is suggested by the lateral variation in strong scattering within the Zwillingsgletscher, which varies by about one-half wavelength, equivalent to 6 months of flow (Nye, 1958; Waddington, 1986). The association of scattering with the crests of ogives, as seen preferentially up glacier, can be explained by accumulation and freezing of water in the autumn and winter versus the melting of ice and filling of crevasses during the summer months (Irvine-Fynn et al., 2011; Fig. 14). We also note that the appearance of deeper scattering “tails” beneath the troughs of the ogives further up glacier (Fig. 6) may represent deeper preserved latent heat release closer to the icefall.

The effect of refreezing on the thermal properties of ice has been noted in other glacier systems. For example, Jania et al. (1996) observed that ice temperatures at 10 m depth in the Hansbreen glacier (Svalbard) are 2–3 °C higher than the mean annual air temperature. They interpreted these elevated ice temperatures as evidence for infiltration and refreezing of meltwater causing a release of latent heat. With particular relevance to this study, Jarvis and Clarke (1974) presented a model whereby water in crevasses can alter the thermal structure of the ice. They showed that the temperature distribution in ice after a glacier surges is modified by the infilling of the new surge-created

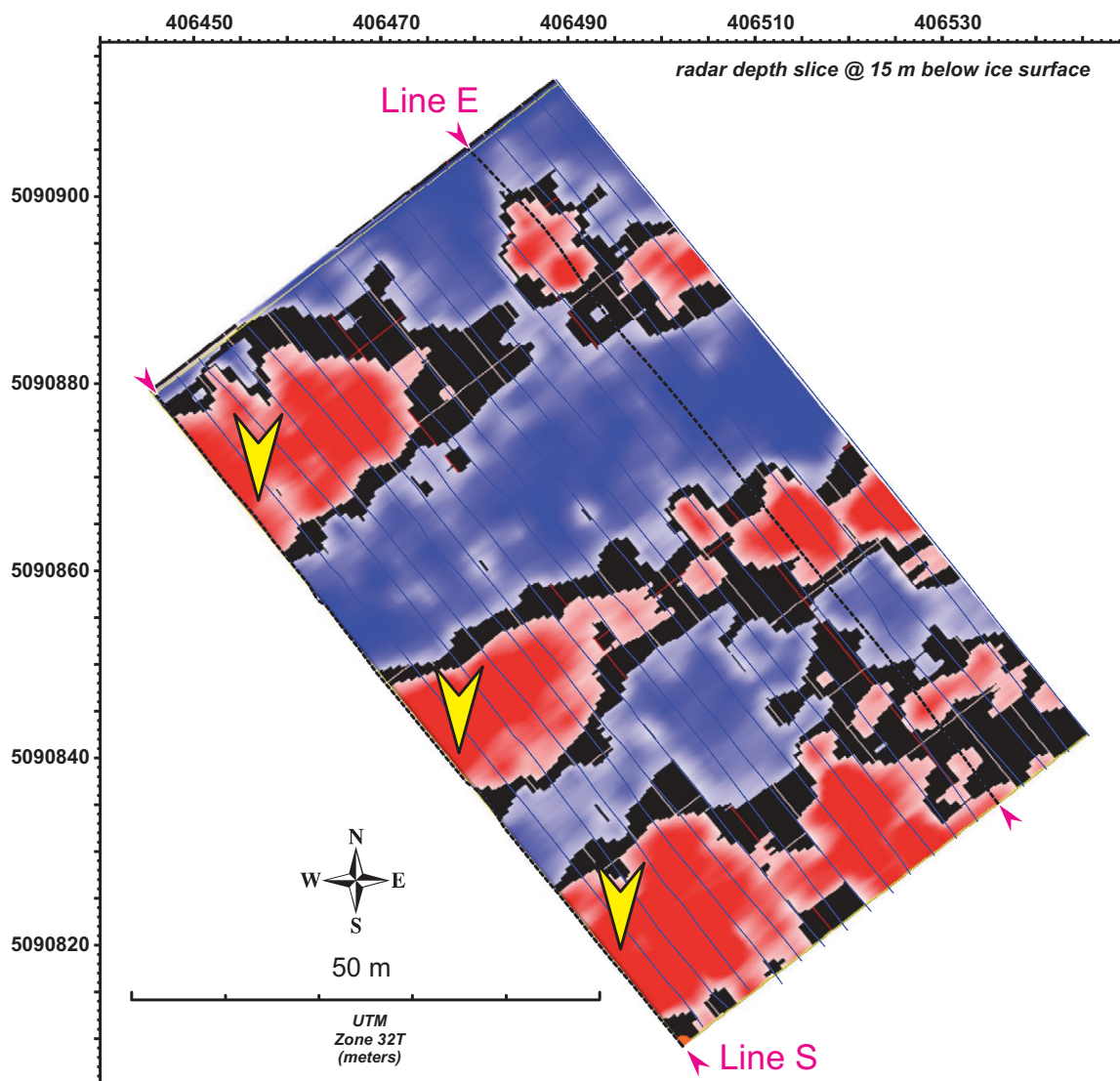


Figure 10. Depth slice (with respect to the ice surface) at 15 m, shown with red colors for high reflectivity and blue as low reflectivity (black is transition between the two extremes). Yellow arrows point out three scattering peaks, as depicted in Figure 9B. Locations of profiles in Figure 9 are noted (see Fig. 1C for location).

crevasses with meltwater that eventually freezes within open crevasses, concentrating thermal energy into a restricted volume. The freezing of water in crevasses results in a latent heat release, creating a locally temperate zone of ice that is advected as the glacier progresses downhill (Jarvis and Clarke, 1974; Irvine-Fynn et al., 2011). Their study indicated that “partially water-filled crevasses can have a significant effect on the temperature distribution within a cold glacier” (Jarvis and Clarke, 1974, p. 252). In particular, they showed that a warm layer of ice could form between 30 and 50 m depth in what is otherwise a cold glacier, which was consistent with their measured subsurface temperatures from the Steele glacier, Yukon Territory, Canada. In

this way, anomalous zones of temperate ice can form that vary laterally along the length of the glacier.

In summary, we suggest that a thick layer of cold ice is advected from the accumulation zone just above the icefall, similar to the situation for the confluence at Grenzletscher (Eisen et al., 2009). In the absence of rapid (<6 month) advection through the icefall, this cold layer will remain unperturbed, and no ogives will form. In the case of the Zwillingsgletscher, the ice moves through the icefall rapidly, thus forming ogives, and simultaneously creating seasonal perturbations in the cold ice at depth through the seasonal freezing of water-filled crevasses (Fig. 14).

SUMMARY AND CONCLUSION

Radar surveys over the Zwillingsgletscher, a narrow tributary of the Gornergletscher system in the Swiss Alps (Canton Valais) with prominent wave ogives, reveal a two-layer ice structure: an upper 5–20-m-thick zone that is transparent to radar that overlies a strongly scattering zone. This well-developed scattering pattern has periodic troughs and ridges (i.e., ridges of high reflectivity laterally alternating with reflection-poor zones) for which the wavelength markedly decreases down glacier. These observations are independent of bare (July) and snow-covered (May) conditions, as surveyed over three field seasons. The onset of strong scattering does not

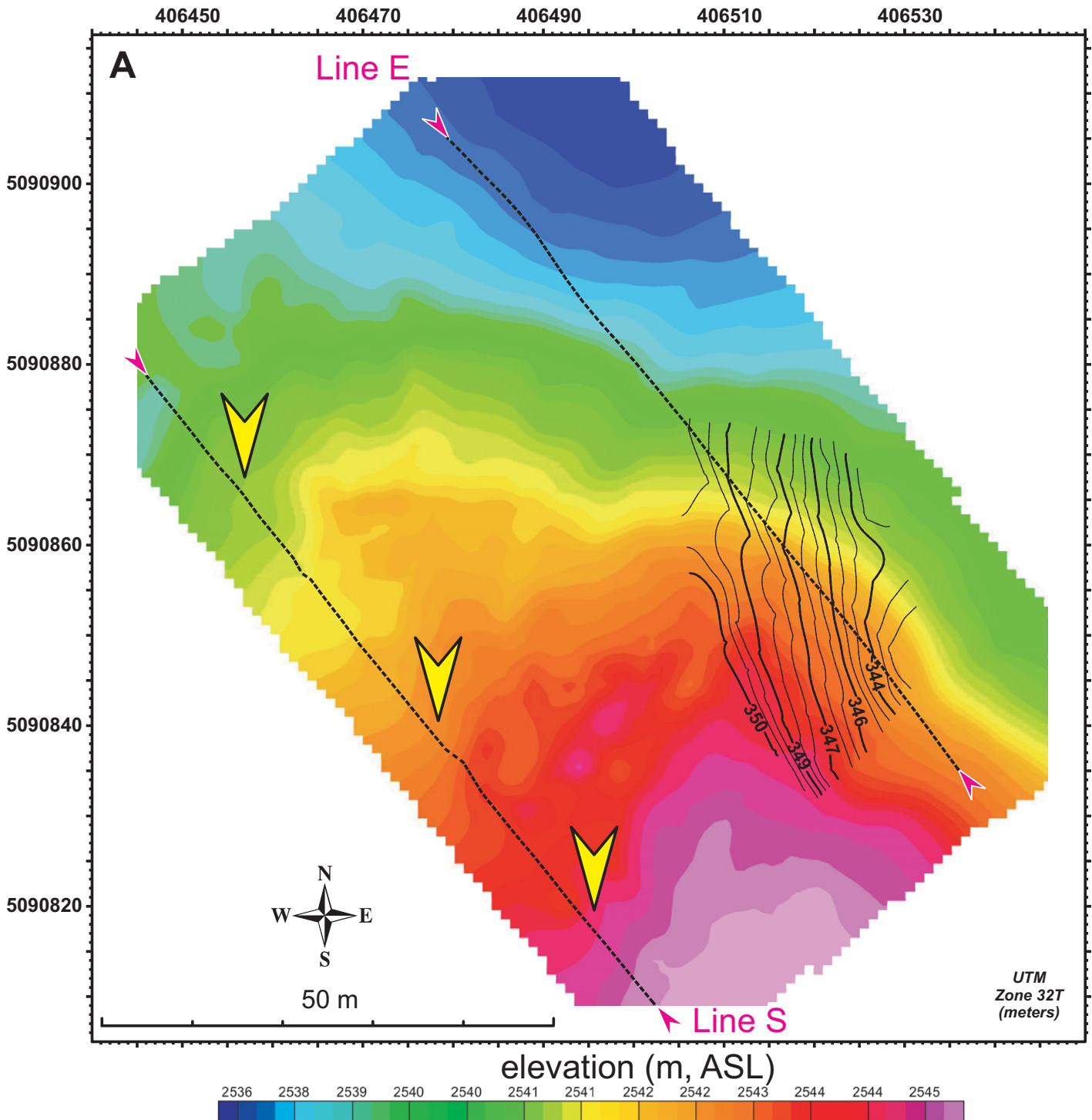


Figure 11 (on this and following two pages). (A) Elevation of ice surface for pseudo-three-dimensional volume area (location of map is same as for Fig. 10). Also shown are depth contours for one of the planar reflectors mapped from the volume (Fig. 9A) (depth contours are expressed as depth below datum = 2870 m above sea level [ASL]). Locations of profiles in Fig. 9 are noted (see Fig. 1C for location). Yellow arrows point out three scattering peaks, as depicted in Fig. 9B.

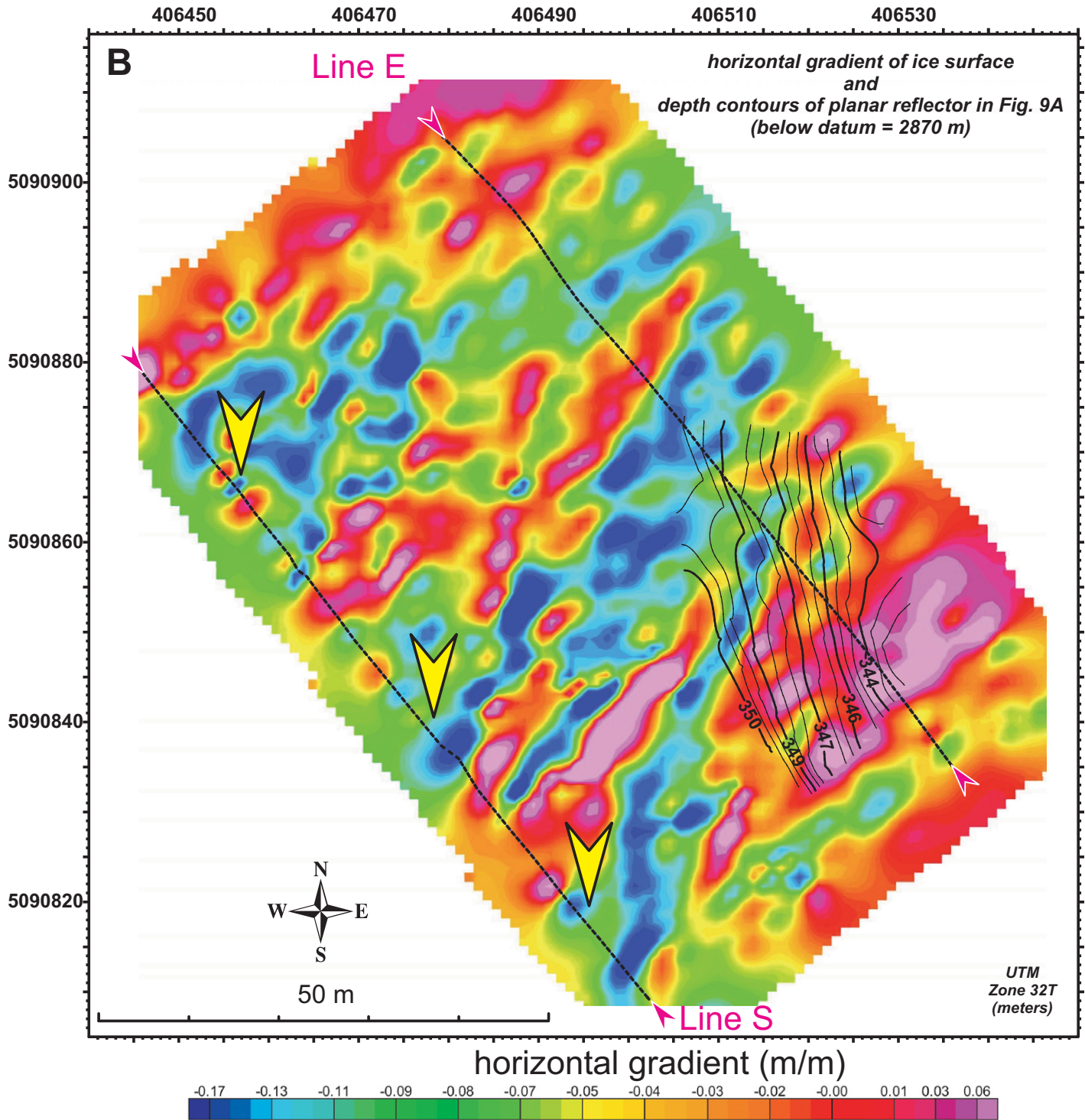


Figure 11 (continued). (B) Same as in A, but a two-dimensional horizontal gradient (referenced to 135° from east) is applied to the elevation data and gridded.

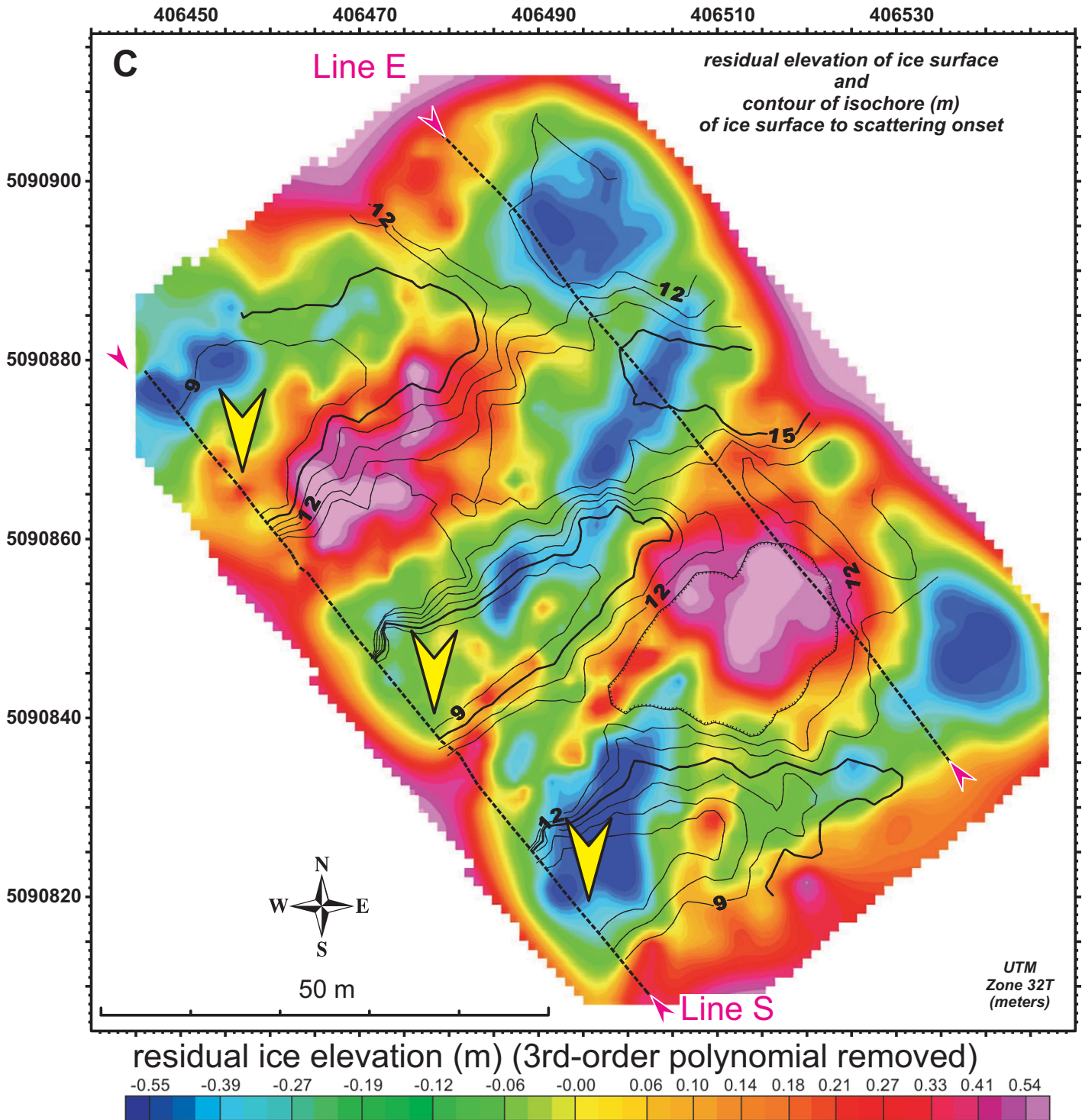
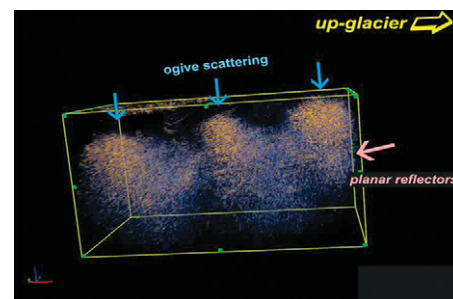


Figure 11 (continued). (C) Same as in A, but showing residual topography (computed by subtracting a third-order polynomial approximation of the elevation data [part A] from the original elevation data) of the ice surface and including isochore (vertical thickness) contours for the interval between the ice surface and the onset of scattering.



Animation 1. Wmv file of volume rendering of amplitudes in the pseudo-three-dimensional (3-D) volume showing complex relation of planar reflectors and scattering peaks. This file can be viewed using Windows Media Player. If you are viewing the PDF of this paper or reading it offline, please visit <http://dx.doi.org/10.1130/GES00804.S1> or the full-text article on www.gsapubs.org to view Animation 1.

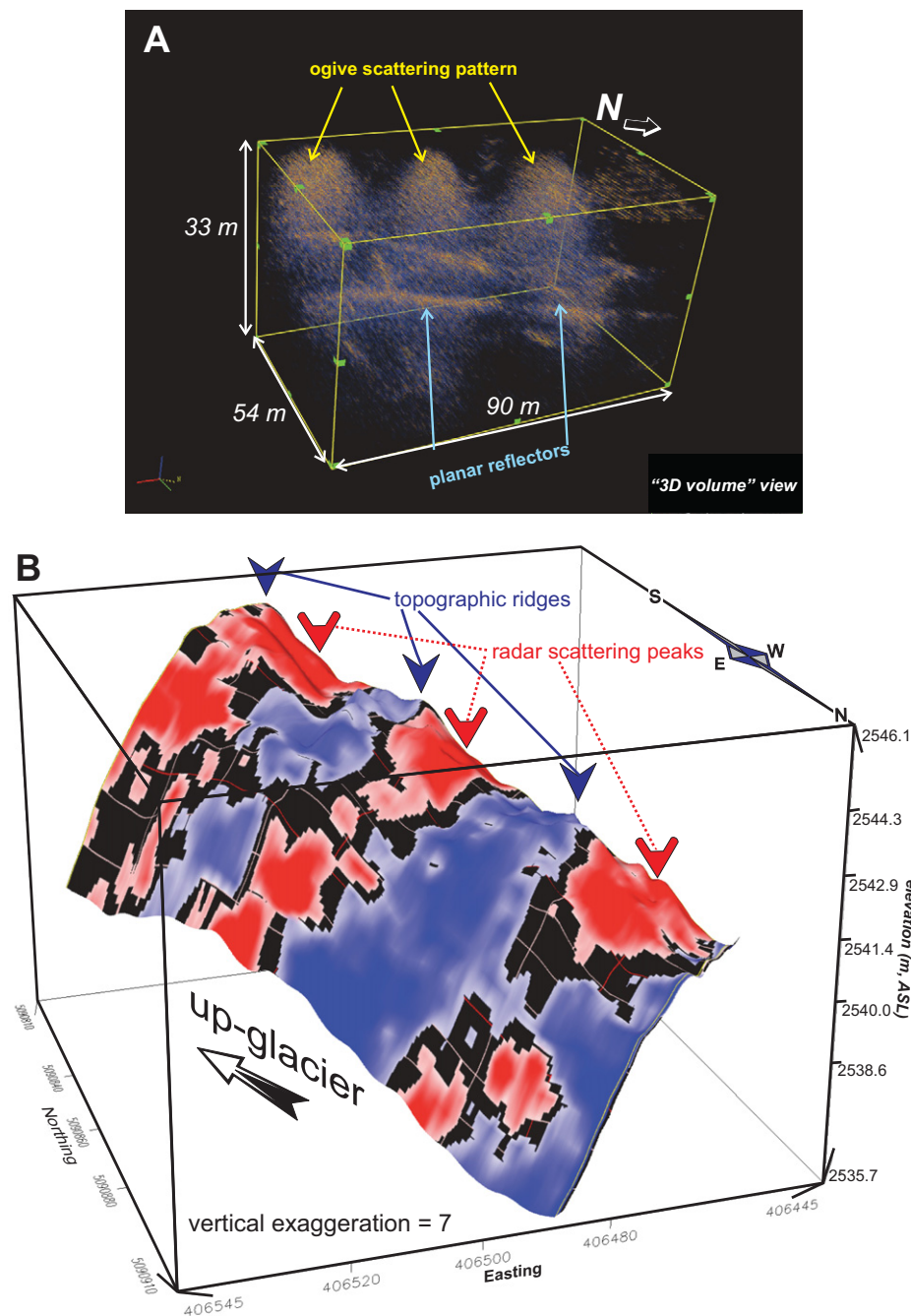


Figure 12. (A) Volume rendering of amplitudes in the pseudo-three-dimensional (3-D) volume (perspective view) showing complex relation of planar reflectors and scattering peaks. See Fig. 1C for location. The relationships depicted in this figure are better viewed in the accompanying video file, available as Animation 1. (B) Radar depth slice from the pseudo-3-D volume in Fig. 10 warped to the ice elevation (vertically exaggerated 7:1) and shown in perspective view. ASL—above sea level.

define a simple surface, but one that includes reflector segments (after migration) as well as an abrupt increase in diffractors. These diffractors are interpreted to represent water-filled voids due to their strong scattering ability. Planar reflectors are also abundantly observed dipping at an oblique angle to the glacial flow direction. The periodicity of the scattering pattern mimics the ogive topography, with the crests of the ogives correlating with the ridges of scattering up glacier. Although this crest-to-ridge correlation drifts out of phase down glacier, the overall periodicity of scattering and ogives is sustained throughout our study area.

Our new observation that spatially links the ice topography and subsurface scattering suggests that a common process governs both the glacier's liquid water content (which likely produces the scattering) and the formation of wave ogives. This linkage also is expressed by the coincident down-glacier reduction in wavelength of the scattering pattern and of the ogive-related topography (Fig. 13). The linkage is further emphasized by the high-precision correlations observed in the down-glacier 3-D survey located where ogive and scattering patterns are less obvious from visual surface observation. The study by Goodsell et al. (2002) of the Bas Glacier d'Arolla is the only other reported case of a periodic radar scattering pattern related to ogives; however, no periodic topography was reported to be associated with the radar pattern. Interestingly, their results show a substantially thinner transparent zone, ~5 m, which may accord with the Bas Glacier d'Arolla having undergone more ablation, so that no obvious topographic (i.e., wave) ogives remain.

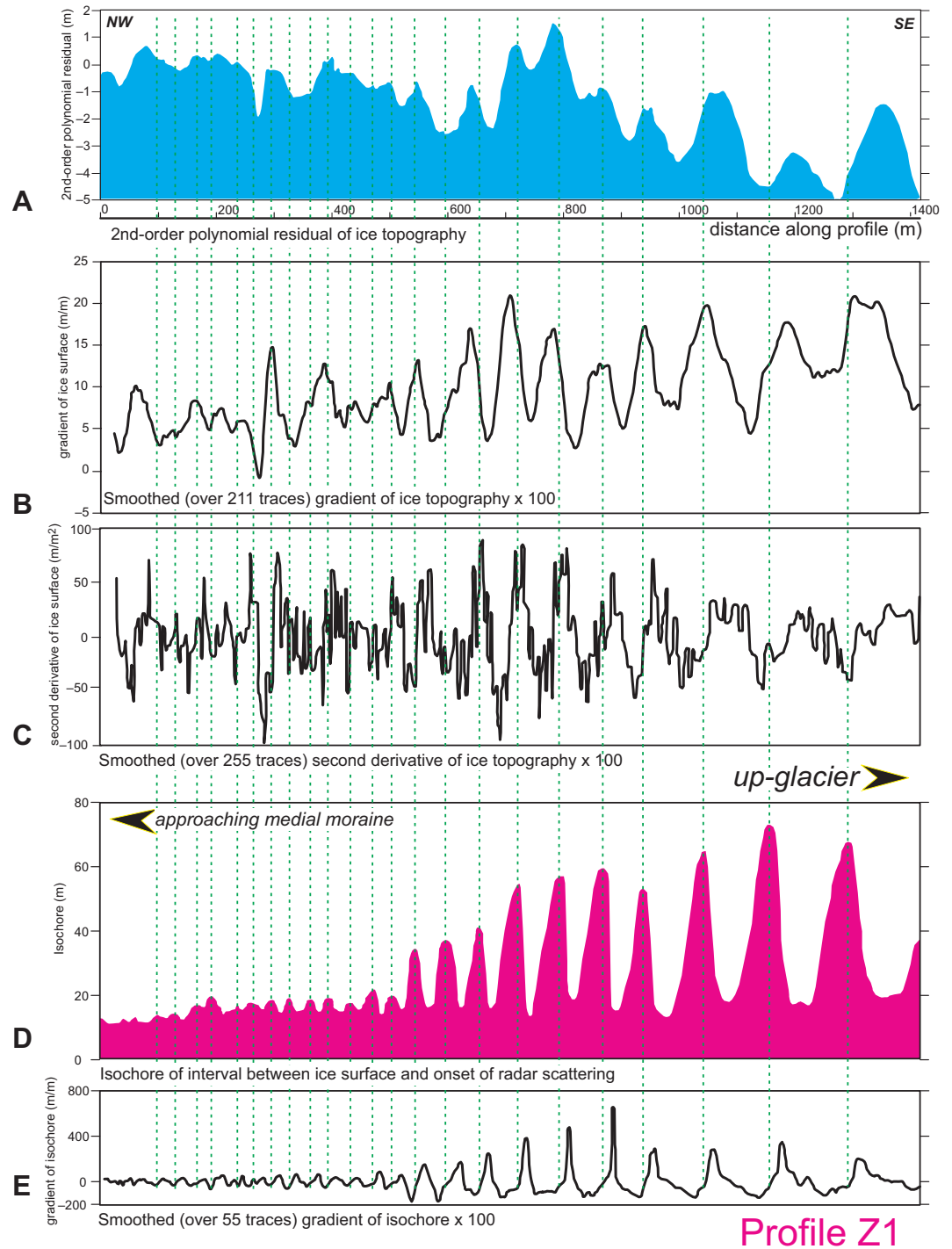


Figure 13 (on this and following page). (A–E) Analysis of the relationship between ice topography (ogives) and the radar scattering periodic patterns for profile Z1 (see Fig. 1C for location). From top to bottom: (A) Residual ice topography computed by subtracting a second-order polynomial approximation from the topography; (B) gradient of the ice surface; (C) second derivative of the ice surface; (D) isochore of the interval between the ice surface and the onset of scattering; and (E) the gradient of the isochore. The amplitude of the isochore in D is interpretive due to the difficulty in uniquely identifying the onset of scattering in the weakly reflective areas (the troughs); however, the peaks are well defined, so that the pattern of the periodicity is robust. Vertical green lines indicate the location of the scattering peaks.

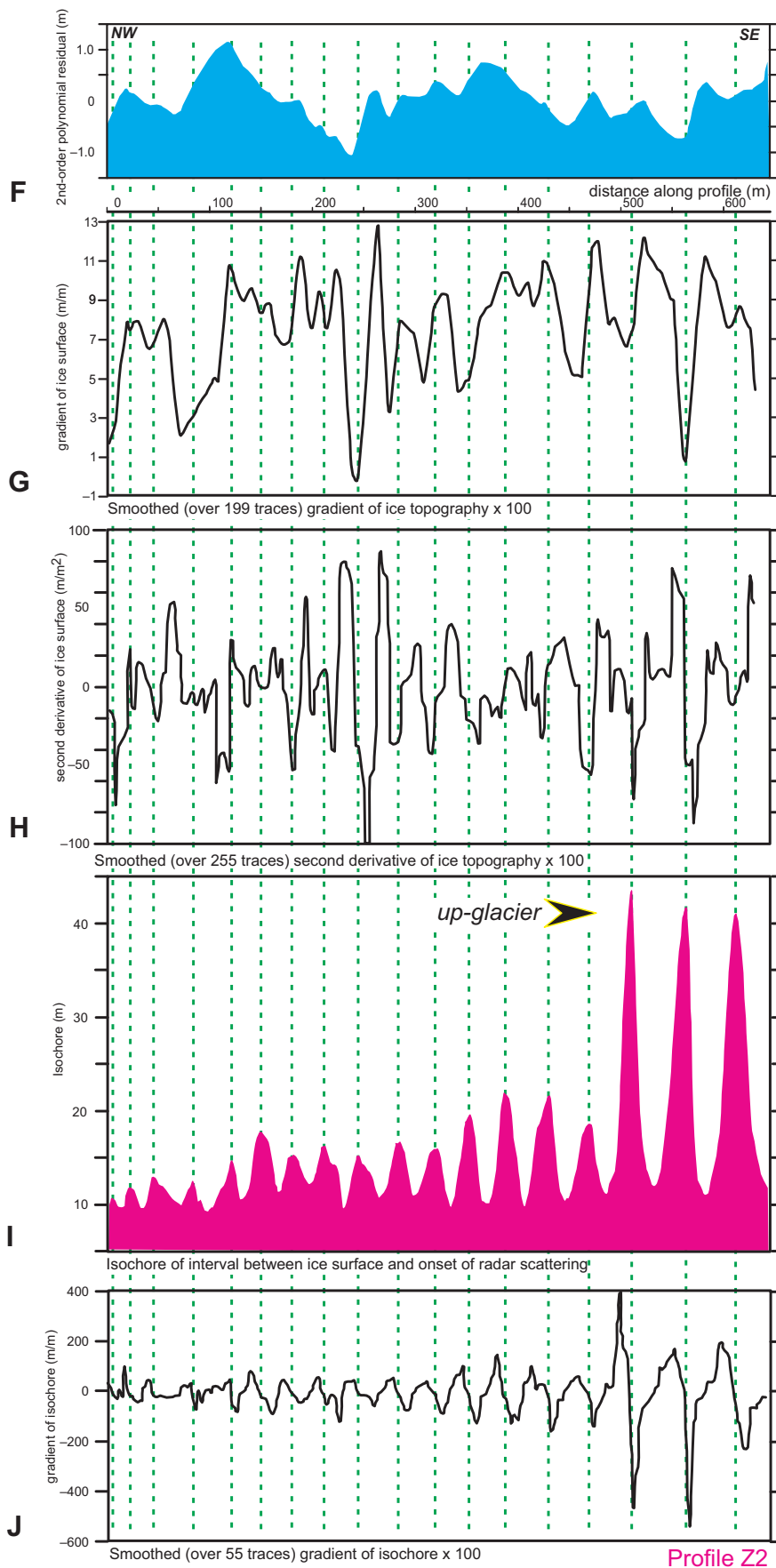
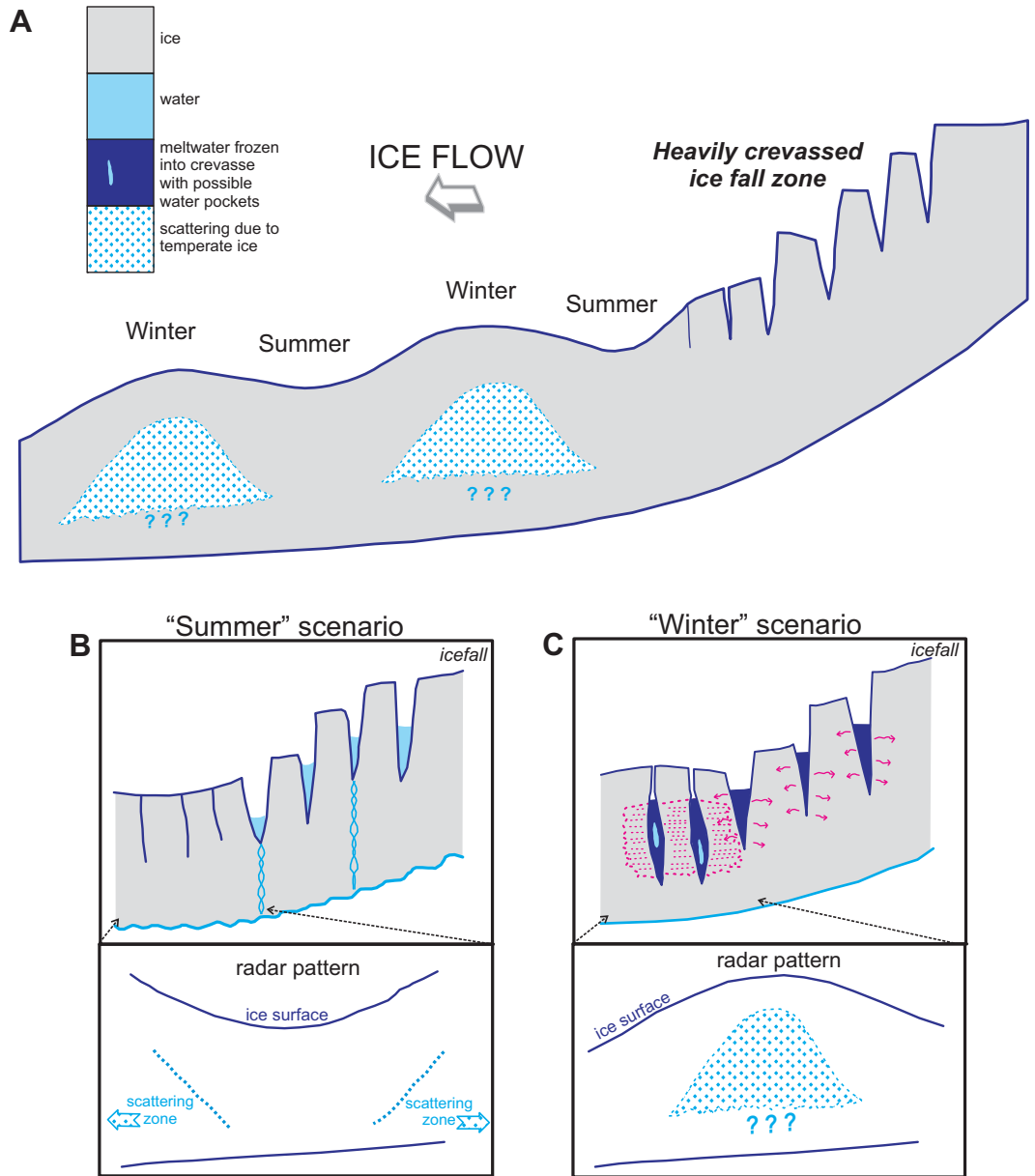


Figure 13 (continued). (F–J) Same as for A–E, but for profile Z2, which is located further to the northwest, where the surface ogive pattern is not as clear.

Figure 14. (A) Idealized cross section of crevassed icefall zone and down-glacier topography and down-glacier topography and radar scattering. “Summer” represents ice that has moved through the icefall zone during summer; “winter” represents ice that has moved through the icefall zone during winter. (B) The “summer” scenario: Crevasses partially fill with water; some drain; no freezing of water; ice remains cold. Stretching and increased ablation result in a topographic low for summer passage of ice. Cold accumulation zone ice remains cold through the icefall and results in low scattering beneath topographic lows. (C) The “winter” scenario: Water-filled crevasses begin to freeze during fall and winter. Some pockets of water may remain. Slower motion through the icefall zone plus increased accumulation result in topographic highs for winter passage of ice. Latent heat release from freezing of water results in warming of the ice. This development of temperate ice during winter plus some liquid water results in high scattering beneath topographic highs. Note: Due to ice deformation, diffusion of heat, and surface ablation over time, the scattering peaks and topographic peaks of the ogives do not necessarily stay in phase as the ice flows down glacier.



The regular, periodic pattern for both the wave ogives and the correlated scattering suggests seasonal variations in temperature and water availability. We propose that surface water infiltrates seasonally in the icefall zone, where the wave ogives develop as the ice accelerates. As this water becomes incorporated into the shallow (upper 50 m) glacier through crevasses or fractures, it freezes in place during the fall and winter months, creating locally temperate ice. This seasonal variation in water infiltration and freezing is manifested as the lateral variation in the radar scattering pattern as the temperate zones are advected down glacier and become progressively compressed and deformed. The presence of water-rich (Murray et al., 2007; Bradford

et al., 2009) zones would have rheological implications for the dynamics of glacial flow (Murray et al., 2007) and englacial water drainage (Fountain et al., 2005). The very different depths to the onset of scattering in the Grenzgletscher (Eisen et al., 2009) and the Zwillingsgletscher suggest different thermal or mechanical flow regimes. Our results support previous conclusions (Goodsell et al., 2002) that glacial ogives are not merely surface features, but likely extend vertically through much of the glacier. Therefore, the extent of ogives at the surface and at depth shows that the Zwillingsgletscher influences a large volume of the main valley glacier, not just the upper surface. As glaciers respond to climatic change (past or future), the thermal structure of

the ice may also change due to variations in ice velocity through icefalls and/or changes in the locations and abundance of crevasses. Future work for the Zwillingsgletscher should include drilling and borehole thermometry in order to penetrate the scattering layer and test these hypotheses for the origin of the scattering and its relation to glacier dynamics.

ACKNOWLEDGMENTS

We gratefully acknowledge support from the National Science Foundation (EAR-0913107). Support was also supplied by the College of Physical and Mathematical Sciences, Brigham Young University. A Mentoring Environment Grant from Brigham Young University supported the involvement of student researchers. Data processing and visualization were

made possible by software grants from the Landmark (Halliburton) University Grant Program and from Seismic Micro-Technology. Reviews of an earlier version of this paper by Steven A. Arcone and an anonymous referee are greatly appreciated and substantially improved the final version.

REFERENCES CITED

- Appleby, J.R., Brook, M.S., Vale, S.S., and Macdonald-Creevey, A., 2010, Structural glaciology of a temperate maritime glacier; Lower Fox glacier, New Zealand: *Geografiska Annaler, ser. A. Physical Geography*, v. 92A, p. 451–467, doi:10.1111/j.1468-0459.2010.00407.x.
- Arcone, S.A., Lawson, D.E., Delaney, A.J., and Moran, M., 2000, 12–100 MHz depth and stratigraphic profiles of temperate glaciers: *SPIE Proceedings Series*, v. 4084, p. 377–382, doi:10.1117/12.383596.
- Bælum, K., and Benn, D.I., 2011, Thermal structure and drainage system of a small valley glacier (Tellbreen, Svalbard), investigated by ground penetrating radar: *Cryosphere*, v. 5, p. 139–149, doi:10.5194/tc-5-139-2011.
- Bamber, J.L., 1987, Internal reflecting horizons in Spitsbergen glaciers: *Annals of Glaciology*, v. 9, p. 5–10.
- Bamber, J.L., 1988, Enhanced radar scattering from water inclusions in ice: *Journal of Glaciology*, v. 34, p. 293–296.
- Björnsson, H., Gjessing, Y., Hamran, S.-E., Hagen, J.O., Liestøl, O.L., Pálsson, F., and Erlingsson, B., 1996, The thermal regime of sub-polar glaciers mapped by multi-frequency radio-echo sounding: *Journal of Glaciology*, v. 42, p. 23–32.
- Bradford, J.H., and Harper, J.T., 2005, Wave field migration as a tool for estimating spatially continuous radar velocity and water content in glaciers: *Geophysical Research Letters*, v. 32, p. L08502, doi:10.1029/2004GL021770.
- Bradford, J.H., Nichols, J., Mikesell, T.D., and Harper, J.T., 2009, Continuous profiles of electromagnetic wave velocity and water content in glaciers: An example from Bench glacier, Alaska, USA: *Annals of Glaciology*, v. 50, p. 1–9, doi:10.3189/172756409789097540.
- Brown, J., Harper, J., and Bradford, J., 2009, A radar transparent layer in a temperate valley glacier: Bench glacier, Alaska: *Earth Surface Processes and Landforms*, v. 34, p. 1497–1506, doi:10.1002/esp.1835.
- Cuffey, K.M., and Paterson, W.S.B., 2010, *The Physics of Glaciers* (4th ed.): Amsterdam, Netherlands, Elsevier, 693 p.
- Eisen, O., Bauder, A., Lüthi, M., Riesen, P., and Funk, M., 2009, Deducing the thermal structure in the tongue of Gornergletscher, Switzerland, from radar surveys and borehole measurements: *Annals of Glaciology*, v. 50, p. 63–70, doi:10.3189/172756409789097612.
- Fisher, J.E., 1962, Ogives of the Forbes type on alpine glaciers and a study of their origins: *Journal of Glaciology*, v. 4, p. 53–61.
- Fountain, A.G., Jacobel, R.W., Schlichting, R., and Jansson, P., 2005, Fractures as the main pathways of water flow in temperate glaciers: *Nature*, v. 433, p. 618–621, doi:10.1038/nature03296.
- Goodsell, B., Hambrey, M.J., and Glasser, N.F., 2002, Formation of band ogives and associated structures at Bas Glacier d’Arolla, Valais, Switzerland: *Journal of Glaciology*, v. 48, p. 287–300, doi:10.3189/172756502781831494.
- Goodsell, B., Hambrey, M.J., Glasser, N.F., Nienow, P., and Mair, D., 2005, The structural glaciology of a temperate valley glacier; Haut Glacier d’Arolla, Valais, Switzerland: Arctic, Antarctic, and Alpine Research, v. 37, p. 218–232, doi:10.1657/1523-0430(2005)037[0218:TSGOAT]2.0.CO;2.
- Gusmeroli, A., Murray, T., Jansson, P., Pettersson, R., Aschwanden, A., and Booth, A.D., 2010, Vertical distribution of water within the polythermal Storgläciären, Sweden: *Journal of Geophysical Research*, v. 115, doi:10.1029/2009JF001539.
- Hambrey, M.J., and Lawson, W., 2000, Structural styles and deformation fields in glaciers: A review, in Maltman, A.J., Hubbard, B., and Hambrey, M.J., eds., *Deformation of Glacial Materials*: Geological Society of London Special Publication 176, p. 59–83.
- Hamran, S.-E., Aarholt, E., Hagen, J.O., and Mo, P., 1996, Estimation of relative water content in a sub-polar glacier using surface-penetration radar: *Journal of Glaciology*, v. 42, p. 533–537.
- Harper, J.T., Bradford, J.H., Humphrey, N.F., and Meierbachtol, T.W., 2010, Vertical extension of the subglacial drainage system into basal crevasses: *Nature*, v. 467, p. 579–582, doi:10.1038/nature09398.
- Irvine-Fynn, T.D.L., Moorman, B.J., Williams, J.L.M., and Walter, F.S.A., 2006, Seasonal changes in ground-penetrating radar signature observed at a polythermal glacier, Bylot Island, Canada: *Earth Surface Processes and Landforms*, v. 31, p. 892–909, doi:10.1002/esp.1299.
- Irvine-Fynn, T.D.L., Hodson, A.J., Moorman, B.J., Vatne, G., and Hubbard, A.L., 2011, Polythermal glacier hydrology: A review: *Reviews of Geophysics*, v. 49, doi:10.1029/2010RG000350.
- Jania, J., Mochacki, D., and Gadek, B., 1996, The thermal structure of Hansbreen, a tidewater glacier in southern Spitsbergen, Svalbard: *Polar Research*, v. 15, p. 53–66, doi:10.1111/j.1751-8369.1996.tb00458.x.
- Jarvis, G.T., and Clarke, G.K.C., 1974, Thermal effects of crevassing on Steele glacier, Yukon Territory, Canada: *Journal of Glaciology*, v. 13, p. 243–254.
- Kadlec, B.J., Tufo, H.M., and Dorn, G.A., 2010, Knowledge-assisted visualization and segmentation of geologic features: *IEEE (Institute of Electrical and Electronics Engineers) Computer Graphics and Applications*, v. 31, no. 1, p. 30–39, doi:10.1109/MCG.2010.13.
- Lawson, D.E., Strasser, J.C., Evenson, E.B., Alley, R.B., Larson, G.J., and Arcone, S.A., 1998, Glaciolydraulic supercooling: A freeze-on mechanism to create stratified, debris-rich basal ice: I. Field evidence: *Journal of Glaciology*, v. 44, p. 547–562.
- Macheret, Y.Y., Otero, J., Navarro, F.J., Vasilenko, E.V., Corcuera, M.I., Cuadrado, M.L., and Glazovsky, A.F., 2009, Ice thickness, internal structure and subglacial topography of Bowles Plateau ice cap and the main ice divides of Livingston Island, Antarctica, by ground-based radio-echo sounding: *Annals of Glaciology*, v. 50, p. 49–56.
- Matsuoka, K., Morse, D., and Raymond, C.F., 2010, Estimating englacial radar attenuation using depth profiles of the returned power, central West Antarctica: *Journal of Geophysical Research*, v. 115, doi:10.1029/2009JF001496.
- McBride, J.H., Rupper, S.B., Ritter, S.M., Tingey, D.G., Quick, A.M., McKean, A.P., and Jones, N.B., 2010, Results of an experimental radar survey on the Gornergletscher glacier system (Zwillingsgletscher), Valais, Switzerland, in *Proceedings of 2010 13th International Conference on Ground Penetrating Radar (GPR)*, 21–25 June 2010: Lecce, Italy, IEEE Xplore Digital Library, p. 1–6, doi:10.1109/ICGPR.2010.5550157.
- Milsom, J.J., 2003, *Field Geophysics* (3rd ed.): West Sussex, UK, John Wiley & Sons Ltd., 232 p.
- Moorman, B.J., and Michel, F.A., 2000, Glacial hydrological system characterisation using ground-penetrating radar: *Hydrological Processes*, v. 14, p. 2645–2667, doi:10.1002/1099-1085(20001030)14:15<2645::AID-HYP84>3.0.CO;2-2.
- Murray, T., Booth, A., and Rippin, D.M., 2007, Water-content of glacier ice: Limitations on estimates from velocity analysis of surface ground penetrating radar surveys: *Journal of Environmental & Engineering Geophysics*, v. 12, p. 87–99, doi:10.2113/JEEG12.1.87.
- Nye, J.F., 1951, The flow of glaciers and ice-sheets as a problem in plasticity: *Proceedings of the Royal Society of London, ser. A. Mathematical and Physical Sciences*, v. 207, p. 554–572, doi:10.1098/rspa.1951.0140.
- Nye, J.F., 1958, A theory of wave formation in glaciers (Cambridge Austerdalsbre Expedition): *Association of International Hydrological Sciences Publication 47, Chamounix Symposium*, p. 139–154.
- Pettersson, R., Jansson, P., and Holmlund, P., 2003, Cold surface layer thinning on Storgläciären, Sweden, observed by repeated ground penetrating radar surveys: *Journal of Geophysical Research*, v. 108, doi:10.1029/2003JF000024.
- Posamentier, H.W., 1978, Thoughts on ogive formation: *Journal of Glaciology*, v. 20, p. 218–220.
- Radzevicius, S.J., Guy, E.D., and Daniels, J.J., 2000, Pitfalls in GPR data interpretation: Differentiating stratigraphy and buried objects from periodic antenna and target effects: *Geophysical Research Letters*, v. 27, p. 3393–3396, doi:10.1029/2000GL008512.
- Sheriff, R.E., and Geldart, L.P., 1995, *Exploration Seismology* (2nd ed.): Cambridge, UK, Cambridge University Press, 592 p.
- Schoof, C., 2010, Ice-sheet acceleration driven by melt supply variability: *Nature*, v. 468, p. 803–806, doi:10.1038/nature09618.
- Waddington, E.D., 1986, Wave ogives: *Journal of Glaciology*, v. 32, p. 325–334.
- Walter, F., Dreger, D.S., Clinton, J.F., Deichmann, N., and Funk, M., 2010, Evidence for near-horizontal tensile faulting at the base of Gornergletscher, a Swiss alpine glacier: *Bulletin of the Seismological Society of America*, v. 100, p. 458–472, doi:10.1785/0120090083.
- White, R., 1991, Properties of instantaneous seismic attributes: *Geophysics: The Leading Edge of Exploration*, v. 10, p. 26–32, doi:10.1190/1.1436827.
- Woodward, J., and Burke, M.J., 2007, Applications of ground-penetrating radar to glacial and frozen materials: *Journal of Environmental & Engineering Geophysics*, v. 12, p. 69–85, doi:10.2113/JEEG12.1.69.